Dilepton production in a rotating thermal medium: The rigid rotation approximation

Jorge David Castaño-Yepes[1,*] and Enrique Muñoz[2,3,†]

[1]*Departamento de Física, Universidad del Valle, Ciudad Universitaria Meléndez, Santiago de Cali 760032, Colombia*

[2]*Facultad de Física, Pontificia Universidad Católica de Chile, Vicuña Mackenna 4860, Santiago, Chile*

[3]*Center for Nanotechnology and Advanced Materials CIEN-UC, Avenida Vicuña Mackenna 4860, Santiago, Chile*

(Received 21 September 2025; accepted 7 May 2026; published 1 June 2026)

We investigate dilepton production in a thermalized quark-gluon plasma subject to global rotation, in the rigid rotating approximation. We consider a generic process involving quark-antiquark annihilation followed by the emission of a highly energetic virtual photon decaying into a dilepton pair. For this process, we compute the dilepton emission rate from the imaginary part of the photon polarization tensor, at finite temperature and vorticity. Our results show that vorticity induces characteristic modifications in the light dilepton channel, namely, e^-e^+ production, where the emission spectrum exhibits a suppression at low transverse mass together with a mild shift of the production threshold. This behavior originates from the role of vorticity as an effective spin-dependent chemical potential that alters the available phase-space distribution for the emission process. In contrast, the $\mu^-\mu^+$ channel is more weakly affected by the rotational background, thus remaining dominated by its intrinsic mass threshold. The resulting channel dependence highlights a potential phenomenological handle for disentangling rotational effects in heavy-ion collisions: while light dilepton spectra encode the imprints of vorticity in the infrared sector, the muon channel provides a comparatively robust baseline.

DOI: 10.1103/fkfs-nlbm

I. INTRODUCTION

As famously stated, *E pur si muove*, attributed to Galileo Galilei [1], even small rotations can induce profound physical consequences. Peripheral heavy-ion collisions provide an unparalleled environment for probing strongly interacting matter under extreme conditions. In particular, such collisions generate ultraintense magnetic fields within the scale of the nuclear overlap region, whose strength increases with the impact parameter and may reach values on the order of the pion mass squared ($\sim 10^{18}$ G) [2–4]. These conditions enable the study of deconfined QCD degrees of freedom in the presence of strong background fields, which in turn give rise to a wide range of novel effects on particle production rates, transport properties, and symmetry-breaking patterns. For a comprehensive review of strongly interacting matter in intense magnetic backgrounds, see Refs. [5,6]. Beyond magnetic fields, the vorticity of the medium formed in noncentral collisions, arising from the spatial anisotropy of the matter distribution in the transverse plane, has emerged as another central aspect of current heavy-ion phenomenology [7–11]. In such systems, it is believed that a well-defined angular velocity $\mathbf{\Omega}$ is produced, with estimates reaching $\sim 10^{22}$ s^{-1} ($\sim$7 MeV) [12]. Unlike the magnetic field, which although extremely strong is short-lived [13], the vorticity is expected to persist throughout the thermal stages of the evolution, particularly within the quark-gluon plasma (QGP). As such, it may decisively shape a variety of observables across both the early and thermalized phases of the collision.

Recent theoretical efforts have incorporated vorticity as a fundamental dynamical ingredient capable of modifying several observables that were previously analyzed in the absence of rotation. For instance, the restoration of chiral symmetry in QCD has been revisited in rotating backgrounds within effective approaches, such as the Yukawa and linear sigma models, where both scalar and fermionic degrees of freedom are influenced by the rotational environment [14,15]. Furthermore, the interplay between magnetic fields and vorticity has attracted significant attention, particularly in relation to their coupled generation

*Contact author: jorge.yepes@correounivalle.edu.co
†Contact author: ejmunozt@uc.cl

Published by the American Physical Society under the terms of the Creative Commons Attribution 4.0 International license. Further distribution of this work must maintain attribution to the author(s) and the published article's title, journal citation, and DOI. Funded by SCOAP³.

mechanisms, as both may arise from the interaction of entropy or charge-density gradients with velocity gradients in the hydrodynamic description of the medium [16]. Vorticity is also expected to impact hadron polarization phenomena, including the global polarization of hyperons and vector mesons, which are considered sensitive probes of the rotational structure of the medium [17–19]. These studies underscore the importance of consistently accounting for vorticity in the dynamical modeling of ultrarelativistic nuclear collisions.

In this work, we focus on dilepton production in a thermalized and rotating QGP. As penetrating electromagnetic probes, dileptons play a central role in current and future experimental programs. Unlike hadrons, whose interactions with the surrounding medium substantially modify their spectral properties, dileptons possess mean free paths that exceed the typical size of the fireball and thus carry essentially undistorted information about the conditions of the plasma from which they originate to the detector [20–22]. The dilepton production rate has been systematically studied within a wide range of theoretical frameworks, incorporating the effects of finite temperature [23–27], static external magnetic fields [28–32], and even fluctuating magnetic backgrounds [33]. Several complementary methods have been used, including the Ritus eigenfunction approach [34], real-time thermal field theory [35], and photon flux techniques [29], among others [36,37].

To establish the role of vorticity in these processes, we analyze the photon polarization tensor in a thermal medium. Previous estimations of the photon polarization tensor in the presence of vorticity were reported in Refs. [19,38], and more recently extensions involving the presence of a magnetic field as well [39]. These computations require analytical expressions for the Fermion propagator in the presence of vorticity, where previous approximations have been presented in [40,41] for open boundary conditions, and an extensive mathematical analysis with different boundary conditions is presented in [42]. In these previous results and approximations, the nonrotating limit is not smoothly connected with the rotating case. Therefore, we shall use here a different approximation for the Fermion propagator, mainly based on the formalism developed by Vilenkin [43], as discussed in detail in Appendix A.

The photon polarization tensor is central to the description of QCD/QED plasmas, as it governs not only the production of dileptons and photons, but also the collective excitations of the medium. Its evaluation has traditionally included thermal and magnetic effects [44–49]. Here, we extend this framework to incorporate a vortical background, aiming to identify its imprints on the dilepton emission rate. Such an analysis is timely in light of recent measurements of polarization and flow-sensitive observables at RHIC and the LHC [12,50], which highlight the need for a systematic theoretical understanding of rotational effects in electromagnetic probes. Our theoretical analysis of the role of vorticity in the dilepton emission rate at finite temperatures, based on the computation of the photon polarization tensor, complements previous results that reported the dilepton yield and elliptic flow in a rotating QGP [38], as well as previous estimations of the dilepton helical rate [51].

The paper is organized as follows. In Sec. II, we present the general formalism connecting the angular-resolved dilepton emission rate with the photon polarization tensor, and we define the coordinate system and approximations assumed for the fermion propagators in a thermal vortical medium. Details on the derivation of the propagator are presented in Appendix A. In Sec. III, we derive our analytical expressions for the photon polarization tensor at finite temperature and vorticity, with additional details provided in Appendices A–D. In Sec. IV, we present our results for the dilepton rates, distinguishing among different fermion-antifermion channels. Finally, in Sec. V, we summarize our findings and outline their phenomenological implications.

II. THEORY

The primary objective of this work is to compute the dilepton emission rate distribution, assuming that the primary nuclear collision generates a local vorticity $\boldsymbol{\Omega} = \hat{z}\Omega$, as depicted in Fig. 1. We thus consider the process represented in Fig. 2, where a quark/antiquark annihilation is followed by a highly energetic virtual photon decaying into a lepton-antilepton pair. Following similar arguments as those discussed in detail in [29], the rate arising from this process is given by the expression

$$\mathcal{R}_{\ell\bar{\ell}} \equiv \frac{d^4R_{\ell\bar{\ell}}}{dp^4} = \frac{\alpha_{\rm em} n_{\rm B}(\omega)}{12\pi^4 M^2}\left(1+\frac{2m_\ell^2}{M^2}\right)\left(1-\frac{4m_\ell^2}{M^2}\right)^{\frac{1}{2}} \mathrm{Im}\,[g_{\mu\nu}\Pi_{\rm R}^{\mu\nu}(\omega)], \tag{1}$$

when $\omega \to \sqrt{M^2+P_T^2}$. Here, $n_{\rm B}(\omega) = (e^{\beta\omega}-1)^{-1}$ denotes the Bose-Einstein distribution at finite temperature, M is the invariant dilepton mass, and $\Pi_{\rm R}^{\mu\nu}(\omega)$ represents the retarded photon polarization tensor that includes all the quark/antiquark possible channels [29]. The geometry shown in Fig. 2 defines the transverse momentum as

$$p_T = \sqrt{p_y^2+p_z^2}, \quad p_y = p_T\cos\phi, \quad p_z = p_T\sin\phi. \tag{2}$$

The longitudinal momentum is expressed in terms of the rapidity

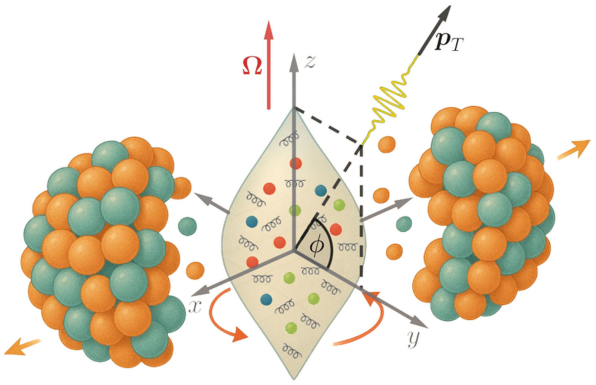


FIG. 1. Coordinate system for the photon's momentum and the local vorticity in the nuclear collision region. Schematic generated using an AI model and Geogebra [52,53].

$$y = \frac{1}{2}\ln\left(\frac{p_0 + p_x}{p_0 - p_x}\right), \tag{3}$$

and, in particular, we focus on the case of midrapidity, $y = 0$ (corresponding to $p_x = 0$).

In the one-loop approximation, the photon polarization tensor due to a virtual quark/antiquark pair of charge q_f, is represented by the Feynman diagram shown in Fig. 3, whose corresponding mathematical expression is given by

$$i\Pi^{\mu\nu} = -\frac{1}{2}\int \frac{d^4k}{(2\pi)^4}\mathrm{Tr}\{iq_f\gamma^\nu iS(k) iq_f\gamma^\mu iS(k-p)\}. \tag{4}$$

A. The Fermion propagator in a rotating frame

We further assume a rotating environment with a constant angular velocity $\mathbf{\Omega}$. The relative tangential velocity of the corotating frame with respect to the laboratory frame is $\mathbf{V} = \mathbf{\Omega} \times \mathbf{R}$. For a choice of the rotation axis such that $\mathbf{\Omega} = \hat{z}\Omega$, as depicted in Fig. 1, the corotating frame is related to the laboratory frame by a system of tetrads (vierbeins) [54] $\{e^a_\mu\}$. Here, $\mu = \hat{0}, \hat{1}, \hat{2}, \hat{3}$ are Minkowski indexes in the laboratory frame, while $a = 0, 1, 2, 3$ are those in the (locally flat) corotating frame. Therefore, we explicitly have

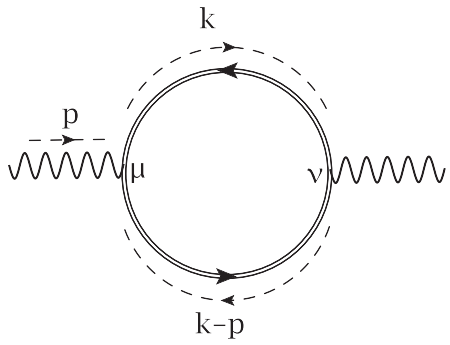


FIG. 3. Feynman diagram illustrating the polarization tensor. The dashed arrows indicate the charge flow in the diagram.

$$e^{\hat{0}}_0 = e^{\hat{1}}_1 = e^{\hat{2}}_2 = e^{\hat{3}}_3 = 1, \qquad e^{\hat{1}}_0 = \Omega y, \qquad e^{\hat{2}}_0 = -\Omega x. \tag{5}$$

The corresponding local metric $g_{\mu\nu} = \eta_{ab}e^a_\mu e^b_\nu$ is given by

$$g_{\mu\nu} = \begin{pmatrix} 1-\Omega^2(x^2+y^2) & \Omega y & -\Omega x & 0 \\ \Omega y & -1 & 0 & 0 \\ -\Omega x & 0 & -1 & 0 \\ 0 & 0 & 0 & -1 \end{pmatrix}. \tag{6}$$

The Dirac matrices in the laboratory frame are defined, in terms of the vierbein, by [55] $\hat{\gamma}^\mu(x) = e^\mu_a\gamma^a$, so that while the γ^a in the local corotating frame satisfy the usual Clifford algebra with the flat Minkowski metric $[\gamma^a, \gamma^b] = 2\eta^{ab}$, those in the laboratory frame satisfy [55] $[\hat{\gamma}^\mu, \hat{\gamma}^\nu] = 2g^{\mu\nu}$.

The Fermion propagator is constructed, as explained in detail in Appendix A, from the free Dirac Lagrangian in the laboratory frame,

$$\mathcal{L} = \bar{\psi}[i\hat{\gamma}^\mu D_\mu - m_f]\psi. \tag{7}$$

Here, in the definition of the covariant derivative $D_\mu \equiv \partial_\mu + \Gamma_\mu$ we included the spin connection [54,55]

$$\Gamma^\mu = -\frac{i}{4}\omega^\mu_{ab}\sigma^{ab}, \tag{8}$$

for $\sigma^{ab} = (i/2)[\gamma^a, \gamma^b]$, and

$$\omega_{\mu ab} \equiv g_{\lambda\rho}e^a_\lambda(\partial_\mu e^\rho_b + \Gamma^\rho_{\mu\nu}e^\nu_b), \tag{9}$$

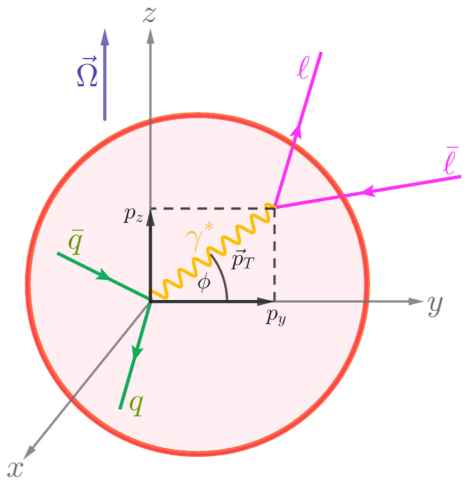


FIG. 2. Feynman diagram and coordinates system for the process of dilepton emission by quark-antiquark annihilation mediated by a virtual photon $q\bar{q} \to \gamma \to l\bar{l}$.

defined after the Christoffel symbols [54]

$$\Gamma^{\lambda}_{\mu\nu} = \frac{1}{2} g^{\lambda\sigma}(\partial_\mu g_{\sigma\nu} + \partial_\nu g_{\mu\sigma} - \partial_\sigma g_{\mu\nu}). \tag{10}$$

As shown in detail in Appendix A, the only nonvanishing component of the spin connection is $\Gamma_{\hat{0}} = -(\mathrm{i}/2)\Omega\sigma^{\hat{1}\hat{2}} = -(\mathrm{i}/2)\boldsymbol{\Omega}\cdot\boldsymbol{\Sigma}$, proportional to the z-component of the spin operator $\boldsymbol{\Sigma}$. The corresponding form of the free Lagrangian, including the finite chemical potential μ, is

$$\mathcal{L} = \bar{\psi}[\mathrm{i}\gamma^a\partial_a + \gamma^0(\Omega J_z + \mu) - m_f]\psi(x), \tag{11}$$

with $\mathbf{J} = \mathbf{L} + \frac{1}{2}\boldsymbol{\Sigma}$ the total angular momentum, involving orbital $\mathbf{L}$ and spin $\frac{1}{2}\boldsymbol{\Sigma}$, respectively.

Therefore, the Fermion propagator is described accordingly, where in the *rigid rotation* approximation developed by us from the Vilenkin formalism [43], as shown in Appendix A, it reads

$$S(p) = \mathcal{O}^{(+)}\frac{\not{p}_+ + m_f}{p_+^2 - m_f^2 + \mathrm{i}\epsilon} + \mathcal{O}^{(-)}\frac{\not{p}_- + m_f}{p_-^2 - m_f^2 + \mathrm{i}\epsilon}. \tag{12}$$

Here, we defined the spin projectors along the direction of the angular velocity, as follows:

$$\mathcal{O}^{(\pm)} = \frac{1}{2}\left(\mathbb{1} \pm \frac{\boldsymbol{\Omega}}{\Omega}\cdot\boldsymbol{\Sigma}\right) = \frac{1}{2}(\mathbb{1} \pm \mathrm{i}\gamma^1\gamma^2) \tag{13a}$$

and

$$p^\mu_\pm \equiv \left(p^0 \pm \frac{\Omega}{2}, \mathbf{p}\right). \tag{13b}$$

We remark that, in the rigid rotating approximation, the angular velocity $\boldsymbol{\Omega}$ plays a role analogous to a spin-dependent chemical potential, and hence it does not break the $SO(3)$ rotational symmetry of the Fermion propagators.

In order to obtain the retarded polarization tensor, as required by the definition of the emission rate Eq. (1), we first compute the diagrams in Matsubara space, and then we perform the standard analytic continuation onto real frequency according to the prescription

$$\Pi^{\mu\nu}_R(p^0 = \omega, \mathbf{p}) = \Pi^{\mu\nu}(\mathrm{i}\nu_n \to \omega + \mathrm{i}\epsilon, \mathbf{p}), \tag{14}$$

where we finally set the external frequency $\omega \to \sqrt{M^2 + p_T^2}$, for M, the invariant dilepton mass.

III. THE PHOTON POLARIZATION TENSOR

As shown in Appendix B, the retarded photon polarization tensor for a quark/antiquark pair with charge q_f and mass m_f takes the form

$$g_{\mu\nu}\Pi^{\mu\nu}_R(\omega) = \frac{q_f^2}{8\pi}\Big[2m_f^2\mathcal{F}(\beta,\omega,\Omega) + [(\omega+\sigma\Omega)^2 - \omega^2]\mathcal{G}(\beta,\omega,\Omega)\Big], \tag{15}$$

where we defined the functions

$$\mathcal{F}(\beta,\omega,\Omega) = \sum_{\sigma,s=\pm1}\int_0^\infty dE f_s(E,\omega)\Delta n_F(E,\omega,\sigma\Omega) \tag{16}$$

and

$$\mathcal{G}(\beta,\omega,\Omega) = \sum_{\sigma,s=\pm1}\int_0^\infty dE f_s(E,\omega+\sigma\Omega)\Delta n_F(E,\omega,\sigma\Omega), \tag{17}$$

respectively. In both expressions above, we defined the functions

$$\Delta n_F(E,\omega,\sigma\Omega) = \omega^{-1}\left\{n_{\mathrm{F}}\left[\beta\left(E - \frac{\sigma\Omega}{2}\right)\right] - n_{\mathrm{F}}\left[\beta\left(E - \omega - \frac{\sigma\Omega}{2}\right)\right]\right\} \tag{18}$$

and

$$f_s(E,\omega) = \Theta(E - m_f)\cdot\{\Theta(E - s\omega - m_f) - \Theta(-E + s\omega - m_f)\}. \tag{19}$$

Here, $n_{\mathrm{F}}(x) = (e^x + 1)^{-1}$ is the Fermi-Dirac distribution, and $\Theta(x)$ is the Heaviside step function. Explicit analytical formulae are obtained for $\mathcal{F}$ [Eq. (C72)] and $\mathcal{G}$ [Eq. (C84)], respectively, but they are quite long so we present them in Appendix C. We also show, in Appendix D, that in the limit $\Omega \to 0$, our analytical expression for the rate reduces to the formula reported by Weldon [56].

Mathematical details, involving evaluation of the sums in Matsubara space and subsequent analytical continuation back to Minkowski space, are presented in Appendices C 1 and C 2.

It is worth emphasizing that the effect of vorticity manifests itself as an effective spin-dependent chemical potential shift, since it only modifies the argument of the Fermi-Dirac distributions.

IV. RESULTS

In Figs. 4 and 5 we show the scaled dilepton production rate, defined as

$$\tilde{\mathcal{R}}_{\ell\ell} \equiv \frac{12\pi^4 M^2}{\alpha_{\mathrm{em}}}\mathcal{R}_{\ell\ell}, \tag{20}$$

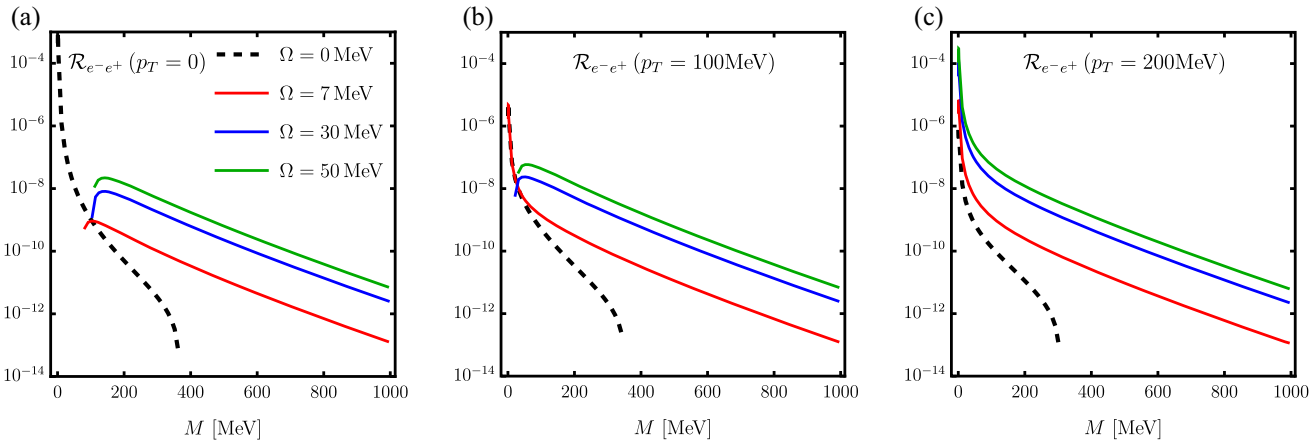


FIG. 4. Electron-positron production rate from Eq. (1) for several values of the vorticity Ω (dashed line $\Omega = 0$, red $\Omega = 7$ MeV, $\Omega = 30$ MeV, $\omega = 50$ MeV) and transverse momentum p_T. The temperature is fixed at $T = 150$ MeV.

plotted as a function of the transverse energy scale $\sqrt{M^2 + p_T^2}$ for several values of vorticity Ω, at a fixed temperature $T = 150$ MeV. The two figures correspond to different production channels: e^-e^+ pairs (Fig. 4) and $\mu^-\mu^+$ pairs (Fig. 5). In each case, the result for $\Omega = 0$, as obtained from our expressions that agree with Ref. [56] in this limit (see Appendix D), is included for comparison. The values of Ω considered extend up to 50 MeV, which is consistent with estimates of the maximum vorticity attainable in heavy-ion collisions without violating causality [57,58]. We thus explore this upper bound as a reference scale for comparison.

For vanishing vorticity, the spectra follow the expected thermal behavior (see Appendix D and Ref. [56]), showing a monotonically decreasing dependence on the transverse energy scale. However, once rotational effects are introduced, clear modifications appear in the light channel e^-e^+, where it is observed that finite values of Ω suppress the dilepton yield in the low-energy region, with the suppression effect becoming monotonically stronger as Ω increases from 7 to 50 MeV. In addition, we clearly identify the presence of a threshold in dilepton production originating from the Heaviside step functions in Eqs. (16) and (17), as defined in Eq. (19).

In the present case, however, the position of this threshold is slightly modified by the vorticity factor, which effectively shifts the argument of the Fermi-Dirac distributions. From a physical standpoint, in the context of the *rigid rotation approximation* adopted in our present analysis, vorticity plays the role of an effective spin-dependent chemical potential associated with the rotational background, thereby redistributing the available phase space for quark-antiquark annihilation. This interpretation naturally explains both the small displacement of the production threshold and the overall suppression of the emission rate at low $\sqrt{M^2 + p_T^2}$. At larger transverse energies the spectra asymptotically converge to the $\Omega = 0$ limit, indicating that the impact of vorticity is mostly confined to the infrared sector. Such behavior is in line with previous analyses of medium-induced modifications to dilepton rates, where the

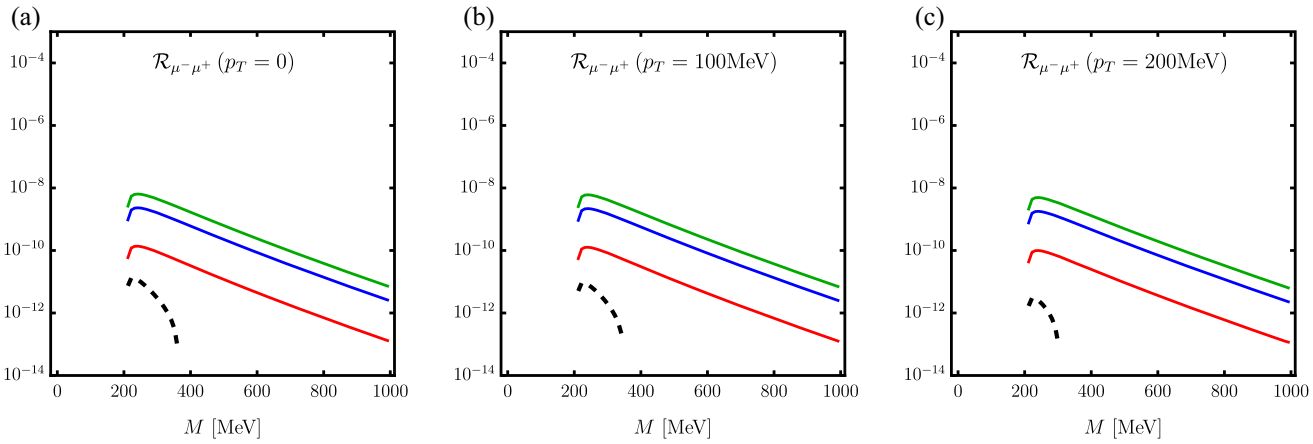


FIG. 5. Muon-antimuon production rates from Eq. (1) for different values of the vorticity Ω (dashed line $\Omega = 0$, red $\Omega = 7$ MeV, $\Omega = 30$ MeV, $\omega = 50$ MeV) and transverse momentum p_T. The temperature is set to $T = 150$ MeV.

dominant effects also manifest themselves at low invariant masses.

The behavior of the $\mu^-\mu^+$ channel, shown in Fig. 5, is qualitatively different. Here, the production rate is dominated by the larger mass threshold, which substantially suppresses the spectrum already in the absence of vorticity. As a result, the relative effect of the rotational background is milder for muon-antimuon pairs than for lighter electron-positron pairs. This example illustrates that heavier dilepton channels are less affected by modifications of the thermal distribution due to vorticity, thus providing a more stable probe of the medium.

Together, these results highlight an important channel dependence in the response of dilepton production to vorticity. Light dilepton channels, namely, the electron-positron channel, display sizable modifications in the low-mass region, while the heavier muon channels have a milder response. From a phenomenological perspective, this difference suggests that experimental measurements of dilepton spectra in heavy-ion collisions could in principle disentangle rotational effects by comparing light and heavy dilepton yields. In particular, any suppression in the low-energy sector of the electron channel relative to the muon channel may serve as an indicator of vorticity in the medium created during the early stages of the collision.

V. SUMMARY AND CONCLUSIONS

In this work we have analyzed dilepton production in a thermalized and rotating quark-gluon plasma by computing the photon polarization tensor at finite temperature and vorticity. This framework allowed us to quantify the role of global rotation in shaping the dilepton emission rate in two different channels, thereby complementing previous studies based on different approximations to the Fermion propagator in a rotating frame [19,38].

Our main findings can be summarized as follows: for the e^-e^+ channel, finite values of the angular velocity Ω lead to a clear suppression of the dilepton yield in the low-mass region, together with a mild displacement of the pair production threshold. These effects can be traced back to the modification of the Fermi distribution functions, as well as the pair production threshold, in the presence of vorticity, which, in the *rigid rotating approximation*, acts as an effective spin-dependent rotational chemical potential redistributing the phase space available for the process. The impact of rotation is more appreciable in the infrared sector of the spectrum, while at larger transverse energy scales (and invariant dilepton masses) the rates converge to their baseline thermal behavior at $\Omega = 0$. By contrast, the heavier $\mu^-\mu^+$ channel shows a milder sensitivity to vorticity, as its production rate is already strongly suppressed by the larger intrinsic mass threshold at $\Omega = 0$.

Together, these results point to a pronounced mass dependence in the response of dilepton production to rotation. From a phenomenological standpoint, this opens an avenue for using comparative analyses of light and heavy dilepton yields as a probe of vorticity in ultra-relativistic nuclear collisions. In particular, a relative suppression of the electron channel in the low-mass region with respect to the muon channel could serve as a signature of rotational effects in the quark-gluon plasma. Such a strategy would complement ongoing efforts to extract information on vorticity from hadronic polarization measurements, while providing an independent electromagnetic probe that is less affected by interactions in the final state.

Looking ahead, we are extending the present analysis going beyond the rigid rotating approximation, by incorporating the effects of the higher angular momentum channels. Moreover, additional ingredients, such as time-dependent vorticity profiles, realistic collective flow dynamics, and the interplay with strong magnetic fields, are under consideration. We are also investigating differential dilepton observables in rapidity and azimuthal angle, which would allow for a more direct comparison with experimental measurements. We are actively seeking these avenues, and this is work in progress that will be presented elsewhere.

ACKNOWLEDGMENTS

J. D. C. Y. would like to thank the Isaac Newton Institute for Mathematical Sciences, Cambridge, for support and hospitality during the programme "Quantum field theory with boundaries, impurities, and defects (BID2025)," where work on this paper was undertaken. This work was supported by EPSRC Grant No. EP/R014604/1. E. M. acknowledges ANID Fondecyt Grant No. 1230440 that supported this work.

DATA AVAILABILITY

The data that support the findings of this article are not publicly available. The data are available from the authors upon reasonable request.

APPENDIX A: THE FERMION PROPAGATOR

As stated in the main text, we assume a rotating frame with a constant angular velocity $\mathbf{\Omega}$. The relative tangential velocity of the corotating frame relative to the laboratory frame is $\mathbf{V} = \mathbf{\Omega} \times \mathbf{R}$. For a choice of the rotation axis such that $\mathbf{\Omega} = \hat{z}\Omega$, as depicted in Fig. 1, the corotating frame is related to the laboratory frame by a system of tetrads (vierbeins) [54] $\{e^a_\mu\}$. Here, $\mu = \hat{0}, \hat{1}, \hat{2}, \hat{3}$ are Minkowski indexes in the laboratory frame, while $a = 0, 1, 2, 3$ are those in the (locally flat) corotating frame. Therefore, we explicitly have [40,42,43]

$$e^{\hat{0}}_0 = e^{\hat{1}}_1 = e^{\hat{2}}_2 = e^{\hat{3}}_3 = 1, \quad e^{\hat{1}}_0 = \Omega y, \quad e^{\hat{2}}_0 = -\Omega x. \tag{A1}$$

The corresponding local metric $g_{\mu\nu} = \eta_{ab} e^a_\mu e^b_\nu$ is given by

$$g_{\mu\nu} = \begin{pmatrix} 1-\Omega^2(x^2+y^2) & \Omega y & -\Omega x & 0 \\ \Omega y & -1 & 0 & 0 \\ -\Omega x & 0 & -1 & 0 \\ 0 & 0 & 0 & -1 \end{pmatrix}. \quad \text{(A2)}$$

The Dirac matrices in the laboratory frame are defined, in terms of the vierbein, by [55] $\hat{\gamma}^\mu(x) = e^\mu_a \gamma^a$, so that while the γ^a in the local corotating frame satisfy the usual Clifford algebra with the flat Minkowski metric [55] $[\gamma^a, \gamma^b] = 2\eta^{ab}$, those in the laboratory frame satisfy $[\hat{\gamma}^\mu, \hat{\gamma}^\nu] = 2g^{\mu\nu}$. The explicit expressions for these matrices are

$$\hat{\gamma}^{\hat{0}} = \gamma^0, \qquad \hat{\gamma}^{\hat{1}} = \Omega y \gamma^0 + \gamma^1,$$
$$\gamma^{\hat{2}} = -\Omega x \gamma^0 + \gamma^2, \qquad \gamma^{\hat{3}} = \gamma^3. \quad \text{(A3)}$$

The Fermion propagator is constructed from the free Dirac Lagrangian in the laboratory frame,

$$\mathcal{L} = \bar{\psi}[\mathrm{i}\hat{\gamma}^\mu D_\mu - m_f]\psi. \quad \text{(A4)}$$

Here, in the definition of the covariant derivative $D_\mu \equiv \partial_\mu + \Gamma_\mu$ we included the spin connection [54,55]

$$\Gamma^\mu = -\frac{\mathrm{i}}{4}\omega^\mu_{ab}\sigma^{ab}, \quad \text{(A5)}$$

for $\sigma^{ab} = (\mathrm{i}/2)[\gamma^a, \gamma^b]$, and

$$\omega_{\mu ab} \equiv g_{\lambda\rho} e^a_\lambda (\partial_\mu e^\rho_b + \Gamma^\rho_{\mu\nu} e^\nu_b), \quad \text{(A6)}$$

defined after the Christoffel symbols [54]

$$\Gamma^\lambda_{\mu\nu} = \frac{1}{2} g^{\lambda\sigma}(\partial_\mu g_{\sigma\nu} + \partial_\nu g_{\mu\sigma} - \partial_\sigma g_{\mu\nu}). \quad \text{(A7)}$$

The explicit analytical expressions for the nonvanishing Christoffel symbols, from Eq. (A2), are

$$\Gamma^{\hat{1}}_{\hat{0}\hat{2}} = \Gamma^{\hat{1}}_{\hat{2}\hat{0}} = -\Omega, \qquad \Gamma^{\hat{2}}_{\hat{0}\hat{1}} = \Gamma^{\hat{2}}_{\hat{1}\hat{0}} = \Omega,$$
$$\Gamma^{\hat{1}}_{\hat{0}\hat{0}} = -\Omega^2 x, \qquad \Gamma^{\hat{2}}_{\hat{0}\hat{0}} = -\Omega^2 y. \quad \text{(A8)}$$

Combining these expressions with the vierbein Eq. (A1), after Eq. (A6) we obtain the only nonvanishing component of the spin connection, $\Gamma_{\hat{0}} = -(\mathrm{i}/2)\Omega\sigma^{\hat{1}\hat{2}} = -(\mathrm{i}/2)\boldsymbol{\Omega}\cdot\boldsymbol{\Sigma}$, which is proportional to the z-component of the spin operator $\boldsymbol{\Sigma}$. The corresponding form of the free Lagrangian density is

$$\mathcal{L} = \bar{\psi}[\mathrm{i}\gamma^a\partial_a + \gamma^0\Omega\hat{J}_z - m_f]\psi(x), \quad \text{(A9)}$$

with $\hat{\mathbf{J}} = \hat{\mathbf{L}} + \frac{1}{2}\hat{\boldsymbol{\Sigma}}$ the total angular momentum, involving orbital $\mathbf{L}$ and spin $\frac{1}{2}\boldsymbol{\Sigma}$, respectively. For this Fermion Lagrangian density, the corresponding Hamiltonian commutes with the set of three operators $\{\hat{P}_z, \hat{J}_z, \hat{W}_0\}$, where $\hat{P}_z$ is the z-component of the linear momentum operator $\hat{\mathbf{P}}$, $\hat{J}_z = \hat{L}_z + \frac{1}{2}\hat{\Sigma}_z = -\mathrm{i}\partial_\varphi + \frac{1}{2}\hat{\Sigma}_z$ is the z-component of the total angular momentum operator, and $\hat{W}_0$ is the 0-component of the Pauli-Lubanski operator [59],

$$\hat{W}_0 = \frac{\hat{\mathbf{P}}\cdot\hat{\mathbf{J}}}{P}, \quad \text{(A10)}$$

whose eigenvalues $h = \pm 1$ represent the helicity components of the spinor eigenfunctions.

The fermion propagator is expressed in terms of the eigenbasis spanned by the solutions to the Dirac equation in rotating coordinates, that after the Lagrangian density Eq. (A9) is

$$\left[\gamma^0(\mathrm{i}\partial_t + \Omega\hat{J}_z + \mathrm{i}\boldsymbol{\gamma}\cdot\nabla - m_f)\right]\hat{\psi}(x) = 0. \quad \text{(A11)}$$

The corresponding spinor solutions, for positive ($\hat{U}$) and negative ($\hat{V}$) energy eigenvalues, are given by [42]

$$\hat{U}_{\alpha_\ell}(x) = \frac{1}{2\pi} e^{-\mathrm{i}\tilde{E}_j t}\hat{u}_{\alpha_\ell}(\mathbf{x}),$$
$$\hat{V}_{\alpha_\ell}(x) = \mathrm{i}\gamma^2\hat{U}^*_{\alpha_\ell}(x) \equiv \frac{1}{2\pi} e^{\mathrm{i}\tilde{E}_j t}\hat{v}_{\alpha_\ell}(\mathbf{x}), \quad \text{(A12)}$$

where we defined $\tilde{E}_j \equiv E - (\ell + 1/2)\Omega$, for $j = \ell + 1/2$ the eigenvalues of $\hat{J}_z$, with $\ell \in \mathbb{Z}$, and the multi-index

$$\alpha_\ell \equiv (E, p_z, \ell, h). \quad \text{(A13)}$$

These eigenfunctions are defined in polar coordinates $\mathbf{x} = (\rho, \varphi, z)$, as follows [42]:

$$\hat{u}_{\alpha_\ell}(\mathbf{x}) = e^{\mathrm{i}p_z z}\begin{pmatrix} \mathcal{C}_{\alpha_\ell +}\phi_{\alpha_\ell}(\rho,\varphi) \\ \mathcal{C}_{\alpha_\ell -}\phi_{\alpha_\ell}(\rho,\varphi) \end{pmatrix}, \quad \text{(A14)}$$

with $\mathcal{C}_{\alpha_\ell \pm}$ normalization coefficients independent of Ω, and the bispinors $\phi_{\alpha_\ell}(\rho,\phi)$ satisfying the differential equation [42]

$$\begin{pmatrix} -\mathrm{i}\partial_\varphi + \frac{1}{2} & 0 \\ 0 & -\mathrm{i}\partial_\varphi - \frac{1}{2} \end{pmatrix}\phi_{\alpha_\ell}(\rho,\phi) = \left(\ell + \frac{1}{2}\right)\phi_{\alpha_\ell}(\rho,\phi), \quad \text{(A15)}$$

so that the spinor solutions are, by definition, also eigenfunctions of the z-component of the total angular momentum operator $\hat{J}_z$ (for $j = \ell + 1/2$),

$$\hat{J}_z\hat{u}_{\alpha_\ell}(\mathbf{x}_1) = j\hat{u}_{\alpha_\ell}(\mathbf{x}_1),$$
$$\hat{J}_z\hat{v}_{\alpha_\ell}(\mathbf{x}_1) = -j\hat{v}_{\alpha_\ell}(\mathbf{x}_1). \tag{A16}$$

The explicit form of these eigenspinors, however not essential for the analysis of the propagator that follows, is constructed in terms of Bessel functions $J_\ell(p_\perp\rho)$ [42],

$$\phi_{\alpha_\ell}(\rho,\varphi) = \frac{1}{\sqrt{2}}\begin{pmatrix} \mathcal{N}_h e^{i\ell\varphi}J_\ell(p_\perp\rho) \\ 2ih\mathcal{N}_{-h}e^{i(\ell+1)\varphi}J_{\ell+1}(p_\perp\rho)\end{pmatrix}, \tag{A17}$$

with the Ω-independent constants $\mathcal{N}_h = (1+2hp_z/p)^{1/2}$, with $p=\sqrt{p_z^2+p_\perp^2}$ being the total linear momentum.

The free-particle propagator, in a rotating system at finite temperature $T=\beta^{-1}$, is expressed by [43]

$$S'(\mathbf{x}_1,\tau_1;\mathbf{x}_2,\tau_2) = \beta^{-1}\sum_n e^{-i\omega_n(\tau_1-\tau_2)}S'(\mathbf{x}_1,\mathbf{x}_2,i\omega_n), \tag{A18}$$

where (in terms of a, b Dirac-spinor components) we have the spectral decomposition [42,43]

$$S'_{ab}(\mathbf{x}_1,\mathbf{x}_2,i\omega_n) = -\sum_{\ell=-\infty}^{\infty}\sum_{h=\pm}\int_{m_f}^{\infty}dE\int_{-p}^{p}dp_z\left(\frac{u^a_{\alpha_\ell}(\mathbf{x}_1)\bar{u}^b_{\alpha_\ell}(\mathbf{x}_2)}{i\omega_n - E + \left(\ell+\frac{1}{2}\right)\Omega} + \frac{v^a_{\alpha_\ell}(\mathbf{x}_1)\bar{v}^b_{\alpha_\ell}(\mathbf{x}_2)}{i\omega_n + E - \left(\ell+\frac{1}{2}\right)\Omega}\right). \tag{A19}$$

Here, $\bar{u}_{\alpha_\ell}(\mathbf{x}) \equiv \hat{u}^\dagger_{\alpha_\ell}(\mathbf{x})\gamma^0$ and $\bar{v}_{\alpha_\ell}(\mathbf{x}) \equiv \hat{v}^\dagger_{\alpha_\ell}(\mathbf{x})\gamma^0$, in the usual notation.

Let us now consider the identity (for $j=\ell+1/2$)

$$\frac{1}{i\omega_n \mp E \pm j\Omega} = \frac{1}{i\omega_n \mp E}\left(1 \pm \frac{j\Omega}{i\omega_n \mp E}\right)^{-1} = \frac{1}{i\omega_n \mp E}\sum_{k=0}^{\infty}\left(\frac{\mp j\Omega}{i\omega_n \mp E}\right)^k. \tag{A20}$$

Therefore, after the eigenvector Eq. (A16), we obtain

$$\begin{aligned}\frac{u^a_{\alpha_\ell}(\mathbf{x}_1)\bar{u}^b_{\alpha_\ell}(\mathbf{x}_2)}{i\omega_n - E + j\Omega} &= \frac{1}{i\omega_n - E}\sum_{k=0}^{\infty}\left(-\frac{j\Omega}{i\omega_n - E}\right)^k u^a_{\alpha_\ell}(\mathbf{x}_1)\bar{u}^b_{\alpha_\ell}(\mathbf{x}_2) \\ &= \frac{1}{i\omega_n - E}\sum_{k=0}^{\infty}\left(\frac{-\hat{J}_z\Omega}{i\omega_n - E}\right)^k u^a_{\alpha_\ell}(\mathbf{x}_1)\bar{u}^b_{\alpha_\ell}(\mathbf{x}_2),\end{aligned} \tag{A21}$$

and similarly

$$\begin{aligned}\frac{v^a_{\alpha_\ell}(\mathbf{x}_1)\bar{v}^b_{\alpha_\ell}(\mathbf{x}_2)}{i\omega_n + E - j\Omega} &= \frac{1}{i\omega_n + E}\sum_{k=0}^{\infty}\left(\frac{j\Omega}{i\omega_n + E}\right)^k v^a_{\alpha_\ell}(\mathbf{x}_1)\bar{v}^b_{\alpha_\ell}(\mathbf{x}_2) \\ &= \frac{1}{i\omega_n + E}\sum_{k=0}^{\infty}\left(\frac{-\hat{J}_z\Omega}{i\omega_n + E}\right)^k v^a_{\alpha_\ell}(\mathbf{x}_1)\bar{v}^b_{\alpha_\ell}(\mathbf{x}_2).\end{aligned} \tag{A22}$$

Therefore, substituting the identities above into Eq. (A19), we obtain

$$S'_{ab}(\mathbf{x}_1,\mathbf{x}_2,i\omega_n) = -\int_{m_f}^{\infty}dE\left[\sum_{k=0}^{\infty}\frac{(-\Omega\hat{J}_z)^k}{(i\omega_n - E)^{k+1}}A_{ab}(\mathbf{x}_1,\mathbf{x}_2) + \sum_{k=0}^{\infty}\frac{(-\Omega\hat{J}_z)^k}{(i\omega_n - E)^{k+1}}B_{ab}(\mathbf{x}_1,\mathbf{x}_2)\right], \tag{A23}$$

where we defined [43]

$$A_{ab}(\mathbf{x}_1,\mathbf{x}_2)=\sum_{\ell}\sum_{h}\int_{-p}^{p}dp_z u^a_{\alpha_\ell}(\mathbf{x}_1)\bar{u}^b_{\alpha_\ell}(\mathbf{x}_2),$$
$$B_{ab}(\mathbf{x}_1,\mathbf{x}_2)=\sum_{\ell}\sum_{h}\int_{-p}^{p}dp_z v^a_{\alpha_\ell}(\mathbf{x}_1)\bar{v}^b_{\alpha_\ell}(\mathbf{x}_2). \tag{A24}$$

Let us notice the operator identity

$$\sum_{k=0}^{\infty}\frac{(-\Omega\hat{J}_z)^k}{(\mathrm{i}\omega_n\pm E)^{k+1}}=\sum_{k=0}^{\infty}(-\Omega\hat{J}_z)^k\frac{(-1)^k}{k!}\frac{\partial^k}{\partial(\mathrm{i}\omega_n)^k}\left(\frac{1}{\mathrm{i}\omega_n\pm E}\right)$$
$$=\exp\left[\Omega\hat{J}_z\frac{\partial}{\partial(\mathrm{i}\omega_n)}\right]\left(\frac{1}{\mathrm{i}\omega_n\pm E}\right). \tag{A25}$$

Therefore, we conclude the exact relation [43]

$$S'(\mathbf{x}_1,\mathbf{x}_2,\mathrm{i}\omega_n)$$
$$=e^{\Omega\hat{J}_z\frac{\partial}{\partial(\mathrm{i}\omega_n)}}\left[-\int_{m_f}^{\infty}dE\left(\frac{A(\mathbf{x}_1,\mathbf{x}_2)}{\mathrm{i}\omega_n-E}+\frac{B(\mathbf{x}_1,\mathbf{x}_2)}{\mathrm{i}\omega_n+E}\right)\right]$$
$$=e^{\Omega\hat{J}_z\frac{\partial}{\partial(\mathrm{i}\omega_n)}}S'_0(\mathbf{x}_1,\mathbf{x}_2,\mathrm{i}\omega_n), \tag{A26}$$

where $S'_0(\mathbf{x}_1,\mathbf{x}_2,\mathrm{i}\omega_n)$ represents the Fermion propagator, in a nonrotating ($\Omega=0$) system, in cylindrical coordinates. On the other hand, we know that the free propagator, in Cartesian coordinates, is given by the expression

$$S_0(\mathbf{x}_1,\mathbf{x}_2,\mathrm{i}\omega_n)=-\int\frac{d^3p}{(2\pi)^3}e^{\mathrm{i}\mathbf{p}\cdot(\mathbf{x}_1-\mathbf{x}_2)}S_0(\mathbf{p},\mathrm{i}\omega_n), \tag{A27}$$

where we defined

$$S_0(\mathbf{p},\mathrm{i}\omega_n)=\frac{\gamma^0(\mathrm{i}\omega_n)-\boldsymbol{\gamma}\cdot\mathbf{p}+m_f}{(\mathrm{i}\omega_n)^2-\mathbf{p}^2-m_f^2} \tag{A28}$$

as the nonrotating ($\Omega=0$) free Fermion propagator in momentum-Matsubara space, with γ^μ Dirac matrices.

Since the polar coordinates (ρ,z,φ) are rotated with respect to the Cartesian coordinates (x,y,z) by an angle φ around the z-axis, the two definitions of the free propagator are mutually related by a unitary transformation, represented by a spinor rotation around the z-axis, i.e., $\hat{U}(\varphi)=\exp(-\mathrm{i}\varphi\hat{J}_z)$, such that

$$S'_0(\mathbf{x}_1,\mathbf{x}_2,\omega_n)=\hat{U}(\varphi_1)S_0(\mathbf{x}_1,\mathbf{x}_2,\omega_n)\hat{U}^\dagger(\varphi_2). \tag{A29}$$

The same relation holds for the rotating propagators in Cartesian $S(\mathbf{x}_1,\mathbf{x}_2,\omega_n)$ and cylindrical $S'(\mathbf{x}_1,\mathbf{x}_2,\omega_n)$ coordinates, respectively, such that by expressing the inverse relation above, we have

$$S(\mathbf{x}_1,\mathbf{x}_2,\omega_n)=\hat{U}^\dagger(\varphi_1)S'(\mathbf{x}_1,\mathbf{x}_2,\omega_n)\hat{U}(\varphi_2)$$
$$=\hat{U}^\dagger(\varphi_1)e^{\Omega\hat{J}_z\frac{\partial}{\partial(\mathrm{i}\omega_n)}}S'_0(\mathbf{x}_1,\mathbf{x}_2,\omega_n)\hat{U}(\varphi_2)$$
$$=e^{\Omega\hat{J}_z\frac{\partial}{\partial(\mathrm{i}\omega_n)}}\hat{U}^\dagger(\varphi_1)S'_0(\mathbf{x}_1,\mathbf{x}_2,\omega_n)\hat{U}(\varphi_2)$$
$$=e^{\Omega\hat{J}_z\frac{\partial}{\partial(\mathrm{i}\omega_n)}}S_0(\mathbf{x}_1,\mathbf{x}_2,\omega_n). \tag{A30}$$

Here, in the last step we used the fact that $[\hat{U}^\dagger(\varphi_1),\hat{J}_z]=0$ to commute the exponential operator, and the unitary property $\hat{U}^\dagger(\varphi)\hat{U}(\varphi)=\hat{U}(\varphi)\hat{U}^\dagger(\varphi)=1$ to solve for $S_0(\mathbf{x}_1,\mathbf{x}_2,\mathrm{i}\omega_n)$ from Eq. (A29). This result can be cast in a more general form, after noticing that $\Omega\hat{J}_z=\boldsymbol{\Omega}\cdot\hat{\mathbf{J}}=\boldsymbol{\Omega}\cdot(\hat{\mathbf{L}}+\frac{1}{2}\hat{\boldsymbol{\Sigma}})$, thus recovering the expression in Eq. (54) of Vilenkin [43],

$$S(\mathbf{x}_1,\mathbf{x}_2,\omega_n)=\exp\left[\boldsymbol{\Omega}\cdot\left(\mathbf{L}+\frac{1}{2}\boldsymbol{\Sigma}\right)\frac{\partial}{\partial(\mathrm{i}\omega_n)}\right]$$
$$\times S_0(\mathbf{x}_1,\mathbf{x}_2,\omega_n). \tag{A31}$$

An important remark about Eq. (A31) is that it trivially reduces, as it should, to the free nonrotating case in the limit $\boldsymbol{\Omega}\to 0$, a property that is clearly not satisfied by the expression reported in Ref. [40]. On the other hand, even though Eq. (A31) is an exact result, it represents only a formal expression, and further algebra and approximations are required to apply it in any practical computation. In order to proceed, we shall first use the expansion of the Fourier exponential in terms of Bessel functions, as follows (for $R=|\mathbf{x}_{\perp,1}-\mathbf{x}_{\perp,2}|$):

$$e^{\mathrm{i}\mathbf{p}\cdot(\mathbf{x}_1-\mathbf{x}_2)}=e^{\mathrm{i}p_z(z_1-z_2)}e^{\mathrm{i}p_\perp R\cos(\varphi_1-\varphi_2)}$$
$$=e^{\mathrm{i}p_z(z_1-z_2)}\sum_{\ell=-\infty}^{\infty}\mathrm{i}^\ell e^{\mathrm{i}\ell(\varphi_1-\varphi_2)}J_\ell(p_\perp R). \tag{A32}$$

Specializing ourselves, as shown in Fig. 1, to a coordinate system with the z-direction parallel to the vorticity $\boldsymbol{\Omega}=\hat{z}\Omega$, we have

$$S(\mathbf{x}_1,\mathbf{x}_2,\mathrm{i}\omega_n)=-\int\frac{d^3p}{(2\pi)^3}e^{[\Omega(\hat{L}_z+\frac{1}{2}\hat{\Sigma}_z)\frac{\partial}{\partial(\mathrm{i}\omega_n)}]}e^{\mathrm{i}\mathbf{p}\cdot(\mathbf{x}_1-\mathbf{x}_2)}S_0(\mathbf{p},\mathrm{i}\omega_n)$$
$$=-\int\frac{d^3p}{(2\pi)^3}e^{\mathrm{i}p_z(z_1-z_2)}\sum_{\ell=-\infty}^{\infty}\mathrm{i}^\ell e^{\mathrm{i}\ell(\varphi_1-\varphi_2)}J_\ell(p_\perp R)e^{[\Omega(\ell+\frac{1}{2}\hat{\Sigma}_z)\frac{\partial}{\partial(\mathrm{i}\omega_n)}]}S_0(\mathbf{p},\mathrm{i}\omega_n), \tag{A33}$$

where we used the fact that $e^{\mathrm{i}\ell(\varphi_1-\varphi_2)}$ are eigenfunctions of $\hat{L}_z=-\mathrm{i}\partial_{\varphi_1}$ with eigenvalue ℓ.

We now introduce the helicity projectors defined in the main text,

$$\hat{\mathcal{O}}^{(\pm)} = \frac{\mathbb{1} \pm \hat{\Sigma}^z}{2}, \tag{A34}$$

in order to perform a spectral decomposition of the exponential operator defined in Eq. (A33) over the subspaces with spin components $+1/2$ and $-1/2$, respectively,

$$\begin{aligned} e^{\left[\Omega\left(\ell+\frac{1}{2}\hat{\Sigma}_z\right)\frac{\partial}{\partial(\mathrm{i}\omega_n)}\right]} S_0(\mathbf{p},\mathrm{i}\omega_n) &= \left[\mathcal{O}^{(+)} e^{\left[\Omega\left(\ell+\frac{1}{2}\right)\frac{\partial}{\partial(\mathrm{i}\omega_n)}\right]} + \mathcal{O}^{(-)} e^{\left[\Omega\left(\ell-\frac{1}{2}\right)\frac{\partial}{\partial(\mathrm{i}\omega_n)}\right]}\right] S_0(\mathbf{p},\mathrm{i}\omega_n) \\ &= \mathcal{O}^{(+)} e^{\left[\Omega\left(\ell+\frac{1}{2}\right)\frac{\partial}{\partial(\mathrm{i}\omega_n)}\right]} S_0(\mathbf{p},\mathrm{i}\omega_n) + \mathcal{O}^{(-)} e^{\left[\Omega\left(\ell-\frac{1}{2}\right)\frac{\partial}{\partial(\mathrm{i}\omega_n)}\right]} S_0(\mathbf{p},\mathrm{i}\omega_n) \\ &= \mathcal{O}^{(+)} S_0\left(\mathbf{p},\mathrm{i}\omega_n + \Omega\left(\ell+\frac{1}{2}\right)\right) + \mathcal{O}^{(-)} S_0\left(\mathbf{p},\mathrm{i}\omega_n + \Omega\left(\ell-\frac{1}{2}\right)\right), \end{aligned} \tag{A35}$$

where in the last step we applied the trivial definition of the differential operator that generates finite translations $\exp(a\partial_x)$,

$$e^{a\partial_x} f(x) = f(x) + a f'(x) + \ldots = \sum_{n=0}^{\infty} \frac{a^n}{n!} f^{(n)}(x) = f(x+a). \tag{A36}$$

By finally inserting Eq. (A35) into Eq. (A33), we obtain the explicit expression for the Fermion operator under rotation $\Omega \neq 0$,

$$\begin{aligned} S(\mathbf{x}_1,\mathbf{x}_2,\mathrm{i}\omega_n) = -\int \frac{d^3p}{(2\pi)^3} e^{\mathrm{i}p_z(z_1-z_2)} \sum_{\ell=-\infty}^{\infty} \mathrm{i}^{\ell} e^{\mathrm{i}\ell(\varphi_1-\varphi_2)} J_{\ell}(p_{\perp}R) \Bigg[\mathcal{O}^{(+)} S_0\left(\mathbf{p},\mathrm{i}\omega_n + \Omega\left(\ell+\frac{1}{2}\right)\right) \\ + \mathcal{O}^{(-)} S_0\left(\mathbf{p},\mathrm{i}\omega_n + \Omega\left(\ell-\frac{1}{2}\right)\right)\Bigg]. \end{aligned} \tag{A37}$$

This last expression is exact, and clearly provides a decomposition into spin $\pm 1/2$ and orbital angular momentum $\ell \in \mathbb{Z}$ channels, with the total angular momentum eigenvalues $j = \ell \pm 1/2$ coupling as a shift in the Matsubara frequencies $\mathrm{i}\omega_n \to \mathrm{i}\omega_n + \Omega j$. We proceed further with an approximation, which is to include in the brackets only the lowest orbital momentum mode $\ell = 0$. Invoking again the identity Eq. (A32), this leads to the approximate form

$$\begin{aligned} S(\mathbf{x}_1,\mathbf{x}_2,\mathrm{i}\omega_n) &= -\int \frac{d^3p}{(2\pi)^3} e^{\mathrm{i}\mathbf{p}\cdot(\mathbf{x}_1-\mathbf{x}_2)} \left[\mathcal{O}^{(+)} S_0\left(\mathbf{p},\mathrm{i}\omega_n + \frac{\Omega}{2}\right) + \mathcal{O}^{(-)} S_0\left(\mathbf{p},\mathrm{i}\omega_n - \frac{\Omega}{2}\right)\right] \\ &\equiv -\int \frac{d^3p}{(2\pi)^3} e^{\mathrm{i}\mathbf{p}\cdot(\mathbf{x}_1-\mathbf{x}_2)} S(\mathbf{p},\mathrm{i}\omega_n), \end{aligned} \tag{A38}$$

where we defined the rotating Fermion propagator in momentum-Matsubara space,

$$\begin{aligned} S(\mathbf{p},\mathrm{i}\omega_n) &\equiv \mathcal{O}^{(+)} S_0\left(\mathbf{p},\mathrm{i}\omega_n + \frac{\Omega}{2}\right) + \mathcal{O}^{(-)} S_0\left(\mathbf{p},\mathrm{i}\omega_n - \frac{\Omega}{2}\right) \\ &= \mathcal{O}^{(+)} \frac{\not{p}_+ + m_f}{p_+^2 - m_f^2} + \mathcal{O}^{(-)} \frac{\not{p}_- + m_f}{p_-^2 - m_f^2}, \end{aligned} \tag{A39}$$

with $p_\sigma = (\mathrm{i}\omega_n + \sigma\Omega/2, \mathbf{p})$, for $\sigma = \pm$ representing the spin projection components.

APPENDIX B: COMPUTATION OF $g_{\mu\nu}\Pi^{\mu\nu}$

From Eq. (4) it is clear that

$$\Pi^{\mu\nu} = \frac{\mathrm{i}q_f^2}{2}\int \frac{d^4k}{(2\pi)^4}\mathrm{Tr}\{\gamma^\nu S(k)\gamma^\mu S(k-p)\}. \quad \text{(B1)}$$

According to the definition, the fermion propagator can be written as

$$S(p) = \mathcal{O}^{(+)}\frac{\not{p}_+ + m_f}{p_+^2 - m_f^2 + \mathrm{i}\epsilon} + \mathcal{O}^{(-)}\frac{\not{p}_- + m_f}{p_-^2 - m_f^2 + \mathrm{i}\epsilon} \quad \text{(B2)}$$

and, similarly,

$$S(k-p) = \mathcal{O}^{(+)}\frac{(\not{k}-\not{p})_+ + m_f}{(k-p)_+^2 - m_f^2 + \mathrm{i}\epsilon} + \mathcal{O}^{(-)}\frac{(\not{k}-\not{p})_- + m_f}{(k-p)_-^2 - m_f^2 + \mathrm{i}\epsilon}, \quad \text{(B3)}$$

where we have defined

$$p_\sigma = \left(p^0 + \sigma\frac{\Omega}{2}, \mathbf{p}\right),$$
$$(k-p)_\sigma = \left(k^0 - p^0 + \sigma\frac{\Omega}{2}, \mathbf{k}-\mathbf{p}\right). \quad \text{(B4)}$$

APPENDIX C: COMPUTATION OF THE DIRAC TRACE

In this section, we explicitly compute the trace over Dirac matrices that is involved in the definition of the photon polarization tensor,

$$\mathrm{Tr}\{\mathrm{i}q_f\gamma^\nu \mathrm{i}S(k)\mathrm{i}q_f\gamma^\mu \mathrm{i}S(q)\}, \quad \text{(C1)}$$

where $q = k - p$, and it is easy to show that the c.c. contribution is given by

$$\mathrm{Tr}\{\mathrm{i}q_f\gamma^\nu \mathrm{i}S(-q)\mathrm{i}q_f\gamma^\mu \mathrm{i}S(-k)\}. \quad \text{(C2)}$$

From the expression of the propagator

$$S(p) = \sum_{s=\pm1}\mathcal{O}^{(s)}\frac{\not{p}_s + m_f}{p_s^2 - m_f^2 + \mathrm{i}\epsilon}, \quad \text{(C3)}$$

we have

$$g_{\mu\nu}[\mathrm{Tr}\{\mathrm{i}q_f\gamma^\nu \mathrm{i}S(k)\mathrm{i}q_f\gamma^\mu \mathrm{i}S(q)\}] = 8q_f^2\left[\frac{m_f^2 - k_+\cdot q_-}{(k_+^2 - m_f^2)(q_-^2 - m_f^2)} + \frac{m_f^2 - k_-\cdot q_+}{(k_-^2 - m_f^2)(q_+^2 - m_f^2)} + \frac{m_f^2}{(k_+^2 - m_f^2)(q_+^2 - m_f^2)} + \frac{m_f^2}{(k_-^2 - m_f^2)(q_-^2 - m_f^2)}\right], \quad \text{(C4)}$$

where $q = k - p$. Therefore, the photon polarization tensor fully contracted with the metric tensor reduces to

$$g_{\mu\nu}\Pi^{\mu\nu}(\omega) = 4q_f^2\sum_{\sigma=\pm1}(\mathcal{I}_\sigma + \mathcal{J}_\sigma), \quad \text{(C5)}$$

where we defined the scalar coefficients

$$\mathcal{I}_\sigma \equiv \mathrm{i}\int \frac{d^4k}{(2\pi)^4}\frac{m_f^2 - k_\sigma\cdot(k-p)_{-\sigma}}{(k_\sigma^2 - m_f^2)[(k-p)_{-\sigma}^2 - m_f^2]} \quad \text{(C6a)}$$

and

$$\mathcal{J}_\sigma \equiv \mathrm{i}\int \frac{d^4k}{(2\pi)^4}\frac{m_f^2}{(k_\sigma^2 - m_f^2)[(k-p)_\sigma^2 - m_f^2]}. \quad \text{(C6b)}$$

1. Matsubara sums

At finite temperature, the temporal component of the momenta is rotated onto the imaginary axis, followed by a discretization in terms of Matsubara frequencies, according to

$$k_0 \to \mathrm{i}\omega_n = \mathrm{i}(2n+1)\pi T,$$
$$p_0 \to \mathrm{i}\nu_l = \mathrm{i}2\pi l T, \quad \text{(C7)}$$

where it is taken into account that k corresponds to the fermionic propagator (odd Matsubara frequencies), whereas p denotes the momentum of the external photon (even Matsubara frequencies).

To perform the Matsubara sum over ω_n, one first identifies the poles of the denominators. There are two distinct types of denominators, namely,

$$(k_\sigma^2 - m_f^2)((k-p)_{-\sigma}^2 - m_f^2) \to \left[(\mathrm{i}\omega_n + \sigma\Omega/2)^2 - E_k^2\right]\left[(\mathrm{i}\omega_n - \mathrm{i}\nu_l - \sigma\Omega/2)^2 - E_{kp}^2\right] \quad \text{(C8a)}$$

and

$$(k_\sigma^2 - m_f^2)((k-p)_\sigma^2 - m_f^2) \to \left[(\mathrm{i}\omega_n + \sigma\Omega/2)^2 - E_k^2\right]\left[(\mathrm{i}\omega_n - \mathrm{i}\nu_l + \sigma\Omega/2)^2 - E_{kp}^2\right]. \quad \text{(C8b)}$$

Here, we have defined

$$E_k \equiv \sqrt{\mathbf{k}^2 + m_f^2},$$
$$E_{kp} \equiv \sqrt{(\mathbf{k}-\mathbf{p})^2 + m_f^2}. \tag{C9}$$

We begin by computing $\mathcal{I}_\sigma$,

$$\mathcal{I}_\sigma \equiv \mathrm{i}\int \frac{d^4k}{(2\pi)^4}\frac{m_f^2 - k_\sigma\cdot(k-p)_{-\sigma}}{(k_\sigma^2 - m_f^2)((k-p)_{-\sigma}^2 - m_f^2)}. \tag{C10}$$

For $k_\sigma\cdot(k-p)_{-\sigma} = (\mathrm{i}\omega_n + \sigma\Omega/2)(\mathrm{i}\omega_n - \mathrm{i}\nu_l - \sigma\Omega/2) - \mathbf{k}\cdot(\mathbf{k}-\mathbf{p})$, this expression can be rewritten as

$$\begin{aligned}\mathcal{I}_\sigma &= \mathrm{i}(\mathrm{i}T)\int\frac{d^3k}{(2\pi)^3}\sum_{n=-\infty}^{+\infty}\frac{m_f^2 - (\mathrm{i}\omega_n + \sigma\Omega/2)(\mathrm{i}\omega_n - \mathrm{i}\nu_l - \sigma\Omega/2) + \mathbf{k}\cdot(\mathbf{k}-\mathbf{p})}{[(\mathrm{i}\omega_n + \sigma\Omega/2)^2 - E_k^2][(\mathrm{i}\omega_n - \mathrm{i}\nu_l - \sigma\Omega/2)^2 - E_{kp}^2]}\\ &= \mathrm{i}\int\frac{d^3k}{(2\pi)^3}S_\sigma^{\mathcal{I}}(E_k, E_{kp}, \Omega).\end{aligned} \tag{C11}$$

The Matsubara sum is evaluated using the standard contour integration method, by choosing a meromorphic function with infinitely many poles at the discrete odd Matsubara frequencies. The Fermi-Dirac distribution fulfills this property. Therefore, we define

$$\begin{aligned}S_\sigma^{\mathcal{I}}(E_k, E_{kp}, \Omega) &= \mathrm{i}T\sum_{n=-\infty}^{+\infty}\frac{m_f^2 - (\mathrm{i}\omega_n + \sigma\Omega/2)(\mathrm{i}\omega_n - \mathrm{i}\nu_l - \sigma\Omega/2) + \mathbf{k}\cdot(\mathbf{k}-\mathbf{p})}{[(\mathrm{i}\omega_n + \sigma\Omega/2)^2 - E_k^2][(\mathrm{i}\omega_n - \mathrm{i}\nu_l - \sigma\Omega/2)^2 - E_{kp}^2]}\\ &= -\mathrm{i}\oint_C\frac{dz}{2\pi\mathrm{i}}\frac{1}{e^{\beta z}+1}\frac{m_f^2 - (z + \sigma\Omega/2)(z - \mathrm{i}\nu_l - \sigma\Omega/2) + \mathbf{k}\cdot(\mathbf{k}-\mathbf{p})}{[(z + \sigma\Omega/2)^2 - E_k^2][(z - \mathrm{i}\nu_l - \sigma\Omega/2)^2 - E_{kp}^2]},\end{aligned} \tag{C12}$$

where C is a contour excluding the imaginary axis, which contains the sequence of simple poles of the Fermi-Dirac distribution $n_{\mathrm{F}}(\beta z) = (e^{\beta z}+1)^{-1}$ at $z_n = \mathrm{i}\omega_n$, and provided by the fact that

$$\mathrm{Res}\left[\frac{-\beta}{e^{\beta z}+1}\right]_{z=\mathrm{i}\omega_n} = 1. \tag{C13}$$

The denominator has four simple poles located at

$$\begin{aligned}z_1 &= -\sigma\frac{\Omega}{2} + E_k,\\ z_2 &= -\sigma\frac{\Omega}{2} - E_k,\\ z_3 &= \sigma\frac{\Omega}{2} - E_{kp} + \mathrm{i}\nu_l,\\ z_4 &= \sigma\frac{\Omega}{2} + E_{kp} + \mathrm{i}\nu_l.\end{aligned} \tag{C14}$$

By Cauchy's theorem, the Matsubara sum can be written as

$$\begin{aligned}S_\sigma^{\mathcal{I}}(E_k, E_{kp}, \Omega) &= -\mathrm{i}\sum_{j=1}^{4} n_{\mathrm{F}}(\beta z_j)\mathrm{Res}\left(\frac{m_f^2 - (z + \sigma\Omega/2)(z - \mathrm{i}\nu_l - \sigma\Omega/2) + \mathbf{k}\cdot(\mathbf{k}-\mathbf{p})}{[(z + \sigma\Omega/2)^2 - E_k^2][(z - \mathrm{i}\nu_l - \sigma\Omega/2)^2 - E_{kp}^2]}\right)_{z=z_j}\\ &= -\mathrm{i}\sum_{s=\pm1}\frac{1}{2E_k}sn_{\mathrm{F}}\left[\beta\left(sE_k - \frac{\sigma\Omega}{2}\right)\right]\frac{m_f^2 - sE_k(sE_k - \sigma\Omega - \mathrm{i}\nu_l) + \mathbf{k}\cdot(\mathbf{k}-\mathbf{p})}{[E_k + E_{kp} - s(\sigma\Omega + \mathrm{i}\nu_l)][E_k - E_{kp} - s(\sigma\Omega + \mathrm{i}\nu_l)]}\\ &\quad -\mathrm{i}\sum_{s=\pm1}\frac{1}{2E_{kp}}sn_{\mathrm{F}}\left[\beta\left(sE_{kp} + \frac{\sigma\Omega}{2} + \mathrm{i}\nu_l\right)\right]\frac{m_f^2 - sE_{kp}(sE_{kp} + \sigma\Omega + \mathrm{i}\nu_l) + \mathbf{k}\cdot(\mathbf{k}-\mathbf{p})}{[E_{kp} + E_k + s(\sigma\Omega + \mathrm{i}\nu_l)][E_{kp} - E_k + s(\sigma\Omega + \mathrm{i}\nu_l)]}.\end{aligned} \tag{C15}$$

Here, $n_{\rm F}(x) \equiv (1+e^x)^{-1}$ is the Fermi-Dirac distribution. For bosonic Matsubara frequencies $i\nu_l = i2\pi l T$, the Fermi distribution satisfies the trivial property

$$n_{\rm F}(\beta(x+i\nu_l)) = n_{\rm F}(\beta x), \tag{C16}$$

which allows the Matsubara sum to be written in the simplified form

$$\begin{aligned} S^{\mathcal{I}}_{\sigma}(E_k, E_{kp}, \Omega) = &-i\sum_{s=\pm1}\frac{1}{2E_k} s n_{\rm F}\left[\beta\left(sE_k - \frac{\sigma\Omega}{2}\right)\right]\frac{m_f^2 - sE_k(sE_k - \sigma\Omega - i\nu_l) + \mathbf{k}\cdot(\mathbf{k}-\mathbf{p})}{[E_k + E_{kp} - s(\sigma\Omega + i\nu_l)][E_k - E_{kp} - s(\sigma\Omega + i\nu_l)]} \\ &- i\sum_{s=\pm1}\frac{1}{2E_{kp}} s n_{\rm F}\left[\beta\left(sE_{kp} + \frac{\sigma\Omega}{2}\right)\right]\frac{m_f^2 - sE_{kp}(sE_{kp} + \sigma\Omega + i\nu_l) + \mathbf{k}\cdot(\mathbf{k}-\mathbf{p})}{[E_{kp} + E_k + s(\sigma\Omega + i\nu_l)][E_{kp} - E_k + s(\sigma\Omega + i\nu_l)]}. \end{aligned} \tag{C17}$$

Returning back to the Minkowski space via analytic continuation $i\nu_l \to \omega + i\epsilon$ (with ω the photon's energy), we obtain

$$\begin{aligned} \mathcal{I}_{\sigma} = &\frac{1}{2}\int\frac{d^3k}{(2\pi)^3}\sum_{s=\pm1} s n_{\rm F}\left[\beta\left(sE_k - \frac{\sigma\Omega}{2}\right)\right]\frac{m_f^2 - sE_k(sE_k - \sigma\Omega - \omega) + \mathbf{k}\cdot(\mathbf{k}-\mathbf{p})}{E_k[E_k + E_{kp} - s(\sigma\Omega + \omega + i\epsilon)][E_k - E_{kp} - s(\sigma\Omega + \omega + i\epsilon)]} \\ &+ \frac{1}{2}\int\frac{d^3k}{(2\pi)^3}\sum_{s=\pm1} s n_{\rm F}\left[\beta\left(sE_{kp} + \frac{\sigma\Omega}{2}\right)\right]\frac{m_f^2 - sE_{kp}(sE_{kp} + \sigma\Omega + \omega) + \mathbf{k}\cdot(\mathbf{k}-\mathbf{p})}{E_{kp}[E_{kp} + E_k + s(\sigma\Omega + \omega + i\epsilon)][E_{kp} - E_k + s(\sigma\Omega + \omega + i\epsilon)]}. \end{aligned} \tag{C18}$$

Furthermore, for on-shell photons with $\mathbf{p}^2 = \omega^2$, we have

$$\mathbf{k}\cdot(\mathbf{p}-\mathbf{k}) = \frac{1}{2}(\omega^2 - E_k^2 - E_{kp}^2 + 2m_f^2), \tag{C19}$$

which allows us to write

$$\begin{aligned} \mathcal{I}_{\sigma} = &\frac{1}{2}\int\frac{d^3k}{(2\pi)^3}\sum_{s=\pm1} s n_{\rm F}\left[\beta\left(sE_k - \frac{\sigma\Omega}{2}\right)\right]\frac{m_f^2 - sE_k(sE_k - \sigma\Omega - \omega) - \frac{1}{2}(\omega^2 - E_k^2 - E_{kp}^2 + 2m_f^2)}{E_k[E_k + E_{kp} - s(\sigma\Omega + \omega + i\epsilon)][E_k - E_{kp} - s(\sigma\Omega + \omega + i\epsilon)]} \\ &+ \frac{1}{2}\int\frac{d^3k}{(2\pi)^3}\sum_{s=\pm1} s n_{\rm F}\left[\beta\left(sE_{kp} + \frac{\sigma\Omega}{2}\right)\right]\frac{m_f^2 - sE_{kp}(sE_{kp} + \sigma\Omega + \omega) - \frac{1}{2}(\omega^2 - E_k^2 - E_{kp}^2 + 2m_f^2)}{E_{kp}[E_{kp} + E_k + s(\sigma\Omega + \omega + i\epsilon)][E_{kp} - E_k + s(\sigma\Omega + \omega + i\epsilon)]}. \end{aligned} \tag{C20}$$

For later convenience, the numerators can be simplified and factored, to obtain the following form:

$$\begin{aligned} \mathcal{I}_{\sigma} = &\frac{1}{2}\int\frac{d^3k}{(2\pi)^3}\sum_{s=\pm1} s n_{\rm F}\left[\beta\left(sE_k - \frac{\sigma\Omega}{2}\right)\right]\frac{-\frac{1}{2}[(sE_k - (\omega + \sigma\Omega))^2 + \omega^2 - (\omega + \sigma\Omega)^2 - E_{kp}^2]}{E_k[E_k + E_{kp} - s(\sigma\Omega + \omega + i\epsilon)][E_k - E_{kp} - s(\sigma\Omega + \omega + i\epsilon)]} \\ &+ \frac{1}{2}\int\frac{d^3k}{(2\pi)^3}\sum_{s=\pm1} s n_{\rm F}\left[\beta\left(sE_{kp} + \frac{\sigma\Omega}{2}\right)\right]\frac{-\frac{1}{2}[(sE_{kp} + \omega + \sigma\Omega)^2 + \omega^2 - (\omega + \sigma\Omega)^2 - E_k^2]}{E_{kp}[E_{kp} + E_k + s(\sigma\Omega + \omega + i\epsilon)][E_{kp} - E_k + s(\sigma\Omega + \omega + i\epsilon)]}. \end{aligned} \tag{C21}$$

We now turn to the computation of $\mathcal{J}_{\sigma}$, defined as

$$\mathcal{J}_{\sigma} \equiv i\int\frac{d^4k}{(2\pi)^4}\frac{m_f^2}{(k_{\sigma}^2 - m_f^2)((k-p)_{\sigma}^2 - m_f^2)}. \tag{C22}$$

By analytic continuation onto Matsubara space, as described in the previous case, and using Eq. (C8b), this expression becomes

$$\mathcal{J}_\sigma = \mathrm{i}(\mathrm{i}T)\int \frac{d^3k}{(2\pi)^3}\sum_{n=-\infty}^{+\infty}\frac{m_f^2}{[(\mathrm{i}\omega_n+\sigma\Omega/2)^2-E_k^2][(\mathrm{i}\omega_n-\mathrm{i}\nu_l+\sigma\Omega/2)^2-E_{kp}^2]}$$
$$= \mathrm{i}\int \frac{d^3k}{(2\pi)^3} S_\sigma^{\mathcal{J}}(E_k,E_{kp},\Omega), \tag{C23}$$

where we defined the Matsubara sum

$$S_\sigma^{\mathcal{J}}(E_k,E_{kp},\Omega) = \mathrm{i}T\sum_{n=-\infty}^{+\infty}\frac{m_f^2}{[(\mathrm{i}\omega_n+\sigma\Omega/2)^2-E_k^2][(\mathrm{i}\omega_n-\mathrm{i}\nu_l+\sigma\Omega/2)^2-E_{kp}^2]}$$
$$= -\mathrm{i}\oint_C \frac{dz}{2\pi\mathrm{i}}\frac{1}{e^{\beta z}+1}\frac{m_f^2}{[(z+\sigma\Omega/2)^2-E_k^2][(z-\mathrm{i}\nu_l+\sigma\Omega/2)^2-E_{kp}^2]}. \tag{C24}$$

Using the same complex contour integration procedure as in the case of $\mathcal{I}_\sigma$, we identify the poles of the integrand at

$$z_1 = -\sigma\frac{\Omega}{2}+E_k,$$
$$z_2 = -\sigma\frac{\Omega}{2}-E_k,$$
$$z_3 = -\sigma\frac{\Omega}{2}-E_{kp}+\mathrm{i}\nu_l,$$
$$z_4 = -\sigma\frac{\Omega}{2}+E_{kp}+\mathrm{i}\nu_l. \tag{C25}$$

The Matsubara sum can then be expressed in terms of the residues at these poles,

$$S_\sigma^{\mathcal{J}}(E_k,E_{kp},\Omega) = -\mathrm{i}\sum_{j=1}^{4} n_{\mathrm{F}}(\beta z_j)\mathrm{Res}\left(\frac{m_f^2}{[(z+\sigma\Omega/2)^2-E_k^2][(z-\mathrm{i}\nu_l+\sigma\Omega/2)^2-E_{kp}^2]}\right)_{z=z_j}$$
$$= -\mathrm{i}\sum_{s=\pm1}\frac{1}{2E_k}sn_{\mathrm{F}}\left[\beta\left(sE_k-\frac{\sigma\Omega}{2}\right)\right]\frac{m_f^2}{(E_k+E_{kp}-s\mathrm{i}\nu_l)(E_k-E_{kp}-s\mathrm{i}\nu_l)}$$
$$-\mathrm{i}\sum_{s=\pm1}\frac{1}{2E_{kp}}sn_{\mathrm{F}}\left[\beta\left(sE_{kp}-\frac{\sigma\Omega}{2}+\mathrm{i}\nu_l\right)\right]\frac{m_f^2}{(E_{kp}+E_k+s\mathrm{i}\nu_l)(E_{kp}-E_k+s\mathrm{i}\nu_l)}. \tag{C26}$$

Applying the identity in Eq. (C16) and performing the analytic continuation $\mathrm{i}\nu_l \to \omega+\mathrm{i}\epsilon$ to real frequency space, we obtain the retarded component,

$$S_\sigma^{\mathcal{J}}(E_k,E_{kp},\Omega) = -\mathrm{i}\sum_{s=\pm1}\frac{1}{2E_k}sn_{\mathrm{F}}\left[\beta\left(sE_k-\frac{\sigma\Omega}{2}\right)\right]\frac{m_f^2}{(E_k+E_{kp}-s(\omega+\mathrm{i}\epsilon))(E_k-E_{kp}-s(\omega+\mathrm{i}\epsilon))}$$
$$-\mathrm{i}\sum_{s=\pm1}\frac{1}{2E_{kp}}sn_{\mathrm{F}}\left[\beta\left(sE_{kp}-\frac{\sigma\Omega}{2}\right)\right]\frac{m_f^2}{(E_{kp}+E_k+s(\omega+\mathrm{i}\epsilon))(E_{kp}-E_k+s(\omega+\mathrm{i}\epsilon))}. \tag{C27}$$

Substituting this result into Eq. (C23) leads to the final expression for $\mathcal{J}_\sigma$,

$$\mathcal{J}_\sigma = \frac{1}{2}\int \frac{d^3k}{(2\pi)^3}\sum_{s=\pm1}sn_{\mathrm{F}}\left[\beta\left(sE_k-\frac{\sigma\Omega}{2}\right)\right]\frac{m_f^2}{E_k(E_k+E_{kp}-s(\omega+\mathrm{i}\epsilon))(E_k-E_{kp}-s(\omega+\mathrm{i}\epsilon))}$$
$$+\frac{1}{2}\int \frac{d^3k}{(2\pi)^3}\sum_{s=\pm1}sn_{\mathrm{F}}\left[\beta\left(sE_{kp}-\frac{\sigma\Omega}{2}\right)\right]\frac{m_f^2}{E_{kp}(E_{kp}+E_k+s(\omega+\mathrm{i}\epsilon))(E_{kp}-E_k+s(\omega+\mathrm{i}\epsilon))}. \tag{C28}$$

2. Momentum integrals

Let us first consider the integral

$$\mathcal{I}_\sigma = \frac{1}{2}\int \frac{d^3k}{(2\pi)^3}\sum_{s=\pm1} s n_{\rm F}\left[\beta\left(sE_k - \frac{\sigma\Omega}{2}\right)\right]\frac{-\frac{1}{2}[(sE_k-(\omega+\sigma\Omega))^2+\omega^2-(\omega+\sigma\Omega)^2-E_{kp}^2]}{E_k[E_k+E_{kp}-s(\sigma\Omega+\omega+i\epsilon)][E_k-E_{kp}-s(\sigma\Omega+\omega+i\epsilon)]}$$
$$+\frac{1}{2}\int \frac{d^3k}{(2\pi)^3}\sum_{s=\pm1} s n_{\rm F}\left[\beta\left(sE_{kp} + \frac{\sigma\Omega}{2}\right)\right]\frac{-\frac{1}{2}[(sE_{kp}+\omega+\sigma\Omega)^2+\omega^2-(\omega+\sigma\Omega)^2-E_{k}^2]}{E_{kp}[E_{kp}+E_k+s(\sigma\Omega+\omega+i\epsilon)][E_{kp}-E_k+s(\sigma\Omega+\omega+i\epsilon)]}. \quad \text{(C29)}$$

Moreover, note that for all the denominators,

$$\frac{1}{[E_k-E_{kp}-s(\sigma\Omega+\omega+i\epsilon)][E_k+E_{kp}-s(\sigma\Omega+\omega+i\epsilon)]}$$
$$=\frac{1}{[\omega+\sigma\Omega+s(E_{kp}-E_k)+i\epsilon][\omega+\sigma\Omega-s(E_k+E_{kp})+i\epsilon]}, \quad \text{(C30)}$$

and similarly,

$$\frac{1}{[E_{kp}-E_k+s(\sigma\Omega+\omega+i\epsilon)][E_{kp}+E_k+s(\sigma\Omega+\omega+i\epsilon)]}$$
$$=\frac{1}{[\omega+\sigma\Omega+s(E_{kp}-E_k)+i\epsilon][\omega+\sigma\Omega+s(E_{kp}+E_k)+i\epsilon]}, \quad \text{(C31)}$$

so that by applying the Plemelj's identity

$$\lim_{\epsilon\to0}\frac{1}{(A+i\epsilon)(B+i\epsilon)} = \text{P.V.}\left(\frac{1}{AB}\right) - i\pi\frac{\delta(A)}{B-A} + i\pi\frac{\delta(B)}{B-A}, \quad \text{(C32)}$$

we get for the imaginary part (which is the only piece necessary to compute the dilepton emission rate)

$$\begin{aligned}\text{Im}[\mathcal{I}_\sigma] = &-\frac{\pi}{8}\sum_{s=\pm1}\int\frac{d^3k}{(2\pi)^3}\frac{n_{\rm F}[\beta(sE_k-\sigma\frac{\Omega}{2})]}{E_{kp}E_k}\left((sE_k-(\omega+\sigma\Omega))^2+\omega^2-(\omega+\sigma\Omega)^2-E_{kp}^2\right)\\
&\times(\delta[\omega+\sigma\Omega+s(E_{kp}-E_k)]-\delta[\omega+\sigma\Omega-s(E_k+E_{kp})])\\
&+\frac{\pi}{8}\sum_{s=\pm1}\int\frac{d^3k}{(2\pi)^3}\frac{n_{\rm F}[\beta(sE_{kp}+\sigma\frac{\Omega}{2})]}{E_kE_{kp}}\left((sE_{kp}+\omega+\sigma\Omega)^2+\omega^2-(\omega+\sigma\Omega)^2-E_k^2\right)\\
&\times(\delta[\omega+\sigma\Omega+s(E_{kp}-E_k)]-\delta[\omega+\sigma\Omega+s(E_{kp}+E_k)]). \quad \text{(C33)}\end{aligned}$$

We remark that, given the support imposed by the two delta functions in the first term: $\omega+\sigma\Omega-sE_k=\pm sE_{kp}$, the corresponding numerator reduces to

$$(sE_k-(\omega+\sigma\Omega))^2-E_{kp}^2+\omega^2-(\omega+\sigma\Omega)^2=\omega^2-(\omega+\sigma\Omega)^2. \quad \text{(C34)}$$

Similarly, the condition imposed by the support of the second pair of delta functions in the second term: $\omega+\sigma\Omega+sE_{kp}=\pm sE_k$, implies that the numerator in this case reduces to

$$(sE_{kp}+\omega+\sigma\Omega)^2-E_k^2+\omega^2-(\omega+\sigma\Omega)^2=\omega^2-(\omega+\sigma\Omega)^2. \quad \text{(C35)}$$

Therefore, extracting this common and momentum-independent factor outside the integrals, we obtain the much simpler expression

$$\begin{aligned}\mathrm{Im}[\mathcal{I}_\sigma] = &-\frac{\pi}{8}[\omega^2-(\omega+\sigma\Omega)^2]\sum_{s=\pm1}\int\frac{d^3k}{(2\pi)^3}\frac{n_{\mathrm{F}}[\beta(sE_k-\sigma\frac{\Omega}{2})]}{E_{kp}E_k}\\ &\times(\delta[\omega+\sigma\Omega+s(E_{kp}-E_k)]-\delta[\omega+\sigma\Omega-s(E_k+E_{kp})])\\ &+\frac{\pi}{8}[\omega^2-(\omega+\sigma\Omega)^2]\sum_{s=\pm1}\int\frac{d^3k}{(2\pi)^3}\frac{n_{\mathrm{F}}[\beta(sE_{kp}+\sigma\frac{\Omega}{2})]}{E_kE_{kp}}\\ &\times\Big(\delta[\omega+\sigma\Omega+s(E_{kp}-E_k)]-\delta[\omega+\sigma\Omega+s(E_{kp}+E_k)]\Big).\end{aligned} \tag{C36}$$

Here, we defined

$$\begin{aligned}E_k &= \sqrt{\mathbf{k}^2+m_f^2}\geq m_f,\\ E_{kp}(\alpha) &= \sqrt{(\mathbf{k}-\mathbf{p})^2+m_f^2} = \sqrt{\mathbf{k}^2+m_f^2+\omega^2-2\omega k\cos\alpha}\geq m_f,\end{aligned} \tag{C37}$$

since the photon momentum is on-shell $|\mathbf{p}|=\omega>0$, and we defined $\mathbf{k}\cdot\mathbf{p}=\omega k\cos\alpha$. In spherical coordinates, we have

$$d^3k = 2\pi\sin\alpha d\alpha k^2dk = 2\pi dx k^2dk, \tag{C38}$$

where we defined the auxiliary variable $x=\cos\alpha$, for $-1\leq x\leq 1$. Therefore, we have

$$\begin{aligned}\mathrm{Im}[\mathcal{I}_\sigma] = &-\frac{\pi}{8(2\pi)^2}[\omega^2-(\omega+\sigma\Omega)^2]\sum_{s=\pm1}\int_0^\infty dkk^2\int_{-1}^1 dx\Bigg\{\frac{n_{\mathrm{F}}[\beta(sE_k-\sigma\frac{\Omega}{2})]}{E_{kp}E_k}\\ &\times(\delta[\omega+\sigma\Omega+s(E_{kp}-E_k)]-\delta[\omega+\sigma\Omega-s(E_k+E_{kp})])\\ &-\frac{n_{\mathrm{F}}[\beta(sE_{kp}+\sigma\frac{\Omega}{2})]}{E_kE_{kp}}(\delta[\omega+\sigma\Omega+s(E_{kp}-E_k)]-\delta[\omega+\sigma\Omega+s(E_{kp}+E_k)])\Bigg\}\\ = &-\frac{\pi}{8(2\pi)^2}[\omega^2-(\omega+\sigma\Omega)^2]\sum_{s=\pm1}\int_0^\infty dk\frac{k^2}{E_k}\int_{-1}^1 dx\Bigg\{\frac{n_{\mathrm{F}}[\beta(sE_k-\sigma\frac{\Omega}{2})]-n_{\mathrm{F}}[\beta(sE_{kp}+\sigma\frac{\Omega}{2})]}{E_{kp}}\\ &\times\delta[\omega+\sigma\Omega+s(E_{kp}-E_k)]\\ &+\frac{n_{\mathrm{F}}[\beta(sE_{kp}+\sigma\frac{\Omega}{2})]-n_{\mathrm{F}}[\beta(-sE_k-\sigma\frac{\Omega}{2})]}{E_{kp}}\delta[\omega+\sigma\Omega+s(E_k+E_{kp})]\Bigg\},\end{aligned} \tag{C39}$$

where in the second step we changed $s\to -s$ in one of the factors.

Let us first consider the support of the delta functions, which we can express as

$$\delta[\omega+\sigma\Omega+s(E_{kp}(x)\mp E_k)] = \frac{\delta(x-x_0^\mp)}{\left|\frac{\partial E_{kp}}{\partial x}\right|}, \tag{C40}$$

where

$$\left|\frac{\partial E_{kp}}{\partial x}\right| = \left|\frac{-2\omega k}{2\sqrt{\mathbf{k}^2+m_f^2+\omega^2-2\omega kx}}\right| = \frac{\omega k}{E_{kp}(x)}, \tag{C41}$$

and $x_0^\mp$ are the roots of the equations,

$$\omega+\sigma\Omega+s(E_{kp}(x_0^\mp)\mp E_k)=0. \tag{C42}$$

Solving for $E_{kp}(x)$, we have

$$E_{kp}(x_0^{\mp}) = \pm E_k - s(\omega + \sigma\Omega) \geq m_f, \tag{C43}$$

so that

$$\begin{aligned}
\mathrm{Im}[\mathcal{I}_\sigma] &= -\frac{\pi}{8(2\pi)^2}[\omega^2 - (\omega+\sigma\Omega)^2]\sum_{s=\pm1}\int_0^\infty dk\frac{k^2}{E_k}\int_{-1}^{1}dx \\
&\times\left(\frac{n_{\mathrm{F}}[\beta(sE_k - \sigma\frac{\Omega}{2})] - n_{\mathrm{F}}[\beta(sE_{kp}(x)+\sigma\frac{\Omega}{2})]}{E_{kp}(x)}\frac{E_{kp}(x_0^-)}{\omega k}\delta(x-x_0^-)\right. \\
&\left.+\frac{n_{\mathrm{F}}[\beta(sE_{kp}(x)+\sigma\frac{\Omega}{2})] - n_{\mathrm{F}}[\beta(-sE_k - \sigma\frac{\Omega}{2})]}{E_{kp}(x)}\frac{E_{kp}(x_0^+)}{\omega k}\delta(x-x_0^+)\right) \\
&= -\frac{\pi}{8(2\pi)^2}[\omega^2 - (\omega+\sigma\Omega)^2]\sum_{s=\pm1}\int_0^\infty dk\frac{k}{E_k} \\
&\times\left(\left\{\frac{n_{\mathrm{F}}[\beta(sE_k - \sigma\frac{\Omega}{2})] - n_{\mathrm{F}}[\beta(sE_k-\omega-\sigma\frac{\Omega}{2})]}{\omega}\right\}\Theta[E_k - s(\omega+\sigma\Omega) - m_f]\right. \\
&\left.-\left\{\frac{n_{\mathrm{F}}[\beta(-sE_k - \sigma\frac{\Omega}{2})] - n_{\mathrm{F}}[\beta(-sE_k-\omega-\sigma\frac{\Omega}{2})]}{\omega}\right\}\Theta[-E_k - s(\omega+\sigma\Omega) - m_f]\right).
\end{aligned} \tag{C44}$$

Finally, since the integrand depends only on the energy $E_k = \sqrt{\mathbf{k}^2 + m^2}$, it is convenient to change the variables for the last integral as follows:

$$\mathbf{k}^2 = E^2 - m_f^2 \Rightarrow \frac{kdk}{E} = dE, \qquad m_f \leq E < \infty, \tag{C45}$$

and making the change $s \to -s$ in the second term, we obtain

$$\begin{aligned}
\mathrm{Im}[\mathcal{I}_\sigma] &= -\frac{\pi}{8(2\pi)^2}[\omega^2 - (\omega+\sigma\Omega)^2]\sum_{s=\pm1}\int_{m_f}^\infty dE\left(\left\{\frac{n_{\mathrm{F}}[\beta(sE - \sigma\frac{\Omega}{2})] - n_{\mathrm{F}}[\beta(sE-\omega-\sigma\frac{\Omega}{2})]}{\omega}\right\}\right. \\
&\left.\times\{\Theta[E - s(\omega+\sigma\Omega) - m_f] - \Theta[-E + s(\omega+\sigma\Omega) - m_f]\}\right).
\end{aligned} \tag{C46}$$

We now turn to the computation of $\mathcal{J}_\sigma$, defined as

$$\begin{aligned}
\mathcal{J}_\sigma &= \frac{1}{2}\int\frac{d^3k}{(2\pi)^3}\sum_{s=\pm1}sn_{\mathrm{F}}\left[\beta\left(sE_k - \frac{\sigma\Omega}{2}\right)\right]\frac{m_f^2}{E_k(E_k+E_{kp}-s(\omega+i\epsilon))(E_k-E_{kp}-s(\omega+i\epsilon))} \\
&+\frac{1}{2}\int\frac{d^3k}{(2\pi)^3}\sum_{s=\pm1}sn_{\mathrm{F}}\left[\beta\left(sE_{kp} - \frac{\sigma\Omega}{2}\right)\right]\frac{m_f^2}{E_{kp}(E_{kp}+E_k+s(\omega+i\epsilon))(E_{kp}-E_k+s(\omega+i\epsilon))}.
\end{aligned} \tag{C47}$$

After extracting the imaginary part from Plemelj's identity, we end up with

$$\begin{aligned}
\mathrm{Im}[\mathcal{J}_\sigma] &= -\frac{\pi}{4}m_f^2\int\frac{d^3k}{(2\pi)^3}\sum_{s=\pm1}\frac{n_{\mathrm{F}}[\beta(sE_k - \frac{\sigma\Omega}{2})]}{E_{kp}E_k}(\delta[\omega - s(E_k - E_{kp})] - \delta[\omega - s(E_k + E_{kp})]) \\
&+\frac{\pi}{4}m_f^2\int\frac{d^3k}{(2\pi)^3}\sum_{s=\pm1}\frac{n_{\mathrm{F}}[\beta(sE_{kp} - \frac{\sigma\Omega}{2})]}{E_kE_{kp}}(\delta[\omega - s(E_k - E_{kp})] - \delta[\omega + s(E_{kp} + E_k)]).
\end{aligned} \tag{C48}$$

As in the previous case of $\mathcal{I}_\sigma$, we shall perform the integral in spherical coordinates, and we shall apply the change of variables defined for the delta functions in Eq. (C41). After some simplifications, the expression reduces to

$$\begin{aligned}\mathrm{Im}[\mathcal{J}_\sigma] = &-\frac{\pi m_f^2}{4(2\pi)^2}\sum_{s=\pm1}\int_0^\infty dk k^2\int_{-1}^1 dx \frac{n_{\mathrm{F}}[\beta(sE_k-\frac{\sigma\Omega}{2})]}{E_{kp}(x)E_k}(\delta[\omega-s(E_k-E_{kp}(x))]-\delta[\omega-s(E_k+E_{kp}(x))])\\ &+\frac{\pi m_f^2}{4(2\pi)^2}\sum_{s=\pm1}\int_0^\infty dk k^2\int_{-1}^1 dx \frac{n_{\mathrm{F}}[\beta(sE_{kp}(x)-\frac{\sigma\Omega}{2})]}{E_kE_{kp}(x)}(\delta[\omega-s(E_k-E_{kp})]-\delta[\omega+s(E_{kp}(x)+E_k)]).\end{aligned} \tag{C49}$$

Distributing the factors, and introducing the change $s\to -s$ in one of the terms, the expression further simplifies to

$$\begin{aligned}\mathrm{Im}[\mathcal{J}_\sigma] = -\frac{m_f^2\pi}{4(2\pi)^2}\sum_{s=\pm1}\int_0^\infty dk\frac{k^2}{E_k}\int_{-1}^1 dx\Bigg\{&\frac{n_{\mathrm{F}}[\beta(sE_k-\frac{\sigma\Omega}{2})]-n_{\mathrm{F}}[\beta(sE_{kp}(x)-\frac{\sigma\Omega}{2})]}{E_{kp}(x)}\delta[\omega+s(E_{kp}(x)-E_k)]\\ &+\frac{n_{\mathrm{F}}[\beta(sE_{kp}(x)-\frac{\sigma\Omega}{2})]-n_{\mathrm{F}}[\beta(-sE_k-\frac{\sigma\Omega}{2})]}{E_{kp}(x)}\delta[\omega+s(E_k+E_{kp}(x))]\Bigg\}.\end{aligned} \tag{C50}$$

We analyze the condition imposed by the deltas,

$$\delta[\omega+s(E_{kp}(x)\mp E_k)] = \frac{\delta(x-x_1^\mp)}{|\frac{\partial E_{kp}}{\partial x}|} = \frac{E_{kp}(x_1^\mp)}{\omega k}\delta(x-x_1^\mp), \tag{C51}$$

where $x_1^\pm$ is defined as the solution to the equation

$$\omega + s(E_{kp}(x_1^\mp)\mp E_k) = 0, \tag{C52}$$

which corresponds to

$$E_{kp}(x_1^\mp) = \pm E_k - s\omega > m_f. \tag{C53}$$

Performing the change of variables as before, and the required substitutions, we end up with the expression

$$\begin{aligned}\mathrm{Im}[\mathcal{J}_\sigma] = -\frac{m_f^2\pi}{4(2\pi)^2}\sum_{s=\pm1}\int_0^\infty dk\frac{k^2}{E_k}\int_{-1}^1 dx\Bigg\{&\frac{n_{\mathrm{F}}[\beta(sE_k-\frac{\sigma\Omega}{2})]-n_{\mathrm{F}}[\beta(sE_{kp}(x)-\frac{\sigma\Omega}{2})]}{E_{kp}(x)}\frac{E_{kp}(x_1^-)}{\omega k}\delta(x-x_1^-)\\ &+\frac{n_{\mathrm{F}}[\beta(sE_{kp}(x)-\frac{\sigma\Omega}{2})]-n_{\mathrm{F}}[\beta(-sE_k-\frac{\sigma\Omega}{2})]}{E_{kp}(x)}\frac{E_{kp}(x_1^+)}{\omega k}\delta(x-x_1^+)\Bigg\}.\end{aligned} \tag{C54}$$

By further substituting the identities

$$\begin{aligned}E_{kp}(x_1^+) &= -E_k - s\omega > m_f,\\ E_{kp}(x_1^-) &= E_k - s\omega > m_f\end{aligned} \tag{C55}$$

in the integral, we arrive at

$$\begin{aligned}\mathrm{Im}[\mathcal{J}_\sigma] = -\frac{m_f^2\pi}{4\omega(2\pi)^2}\sum_{s=\pm1}\int_0^\infty dk\frac{k}{E_k}\Bigg\{&\left(n_{\mathrm{F}}\left[\beta\left(sE_k-\frac{\sigma\Omega}{2}\right)\right]-n_{\mathrm{F}}\left[\beta\left(sE_k-\omega-\frac{\sigma\Omega}{2}\right)\right]\right)\Theta[E_k-s\omega-m_f]\\ &+\left(n_{\mathrm{F}}\left[\beta\left(-sE_k-\frac{\sigma\Omega}{2}-\omega\right)\right]-n_{\mathrm{F}}\left[\beta\left(-sE_k-\frac{\sigma\Omega}{2}\right)\right]\right)\Theta[-E_k-s\omega-m_f]\Bigg\}.\end{aligned} \tag{C56}$$

Introducing the change $s \to -s$ in the second term, and making the change of variables defined in Eq. (C45), we arrive at

$$\mathrm{Im}[\mathcal{J}_\sigma] = -\frac{m_f^2\pi}{4(2\pi)^2}\sum_{s=\pm1}\int_{m_f}^{\infty} dE\left\{\frac{n_{\mathrm{F}}[\beta(sE-\frac{\sigma\Omega}{2})]-n_{\mathrm{F}}[\beta(sE-\omega-\frac{\sigma\Omega}{2})]}{\omega}\right\} \times\Big\{\Theta[E-s\omega-m_f]-\Theta[-E+s\omega-m_f]\Big\}. \tag{C57}$$

Collecting both contributions, we arrive at the final result

$$\begin{aligned}\mathrm{Im}\left[g_{\mu\nu}\Pi_R^{\mu\nu}(\omega)\right] &= 4q_f^2\sum_{\sigma=\pm1}(\mathrm{Im}[\mathcal{I}_\sigma]+\mathrm{Im}[\mathcal{J}_\sigma]) \\ &= \frac{q_f^2}{8\pi}[2m_f^2\mathcal{F}(\beta,\omega,\Omega)+[(\omega+\sigma\Omega)^2-\omega^2]\mathcal{G}(\beta,\omega,\Omega)],\end{aligned} \tag{C58}$$

where we defined the functions

$$\mathcal{F}(\beta,\omega,\Omega) = \sum_{\sigma=\pm1}\sum_{s=\pm1}\int_{m_f}^{\infty} dE\Delta n_F(sE,\omega,\sigma\Omega)\Big\{\Theta[E-s\omega-m_f]-\Theta[-E+s\omega-m_f]\Big\}, \tag{C59}$$

and

$$\mathcal{G}(\beta,\omega,\Omega) = \sum_{\sigma=\pm1}\sum_{s=\pm1}\int_{m_f}^{\infty} dE\Delta n_F(sE,\omega,\sigma\Omega)\Big\{\Theta[E-s(\omega+\sigma\Omega)-m_f]-\Theta[-E+s(\omega+\sigma\Omega)-m_f]\Big\}, \tag{C60}$$

with

$$\Delta n_F(sE,\omega,\sigma\Omega) = \frac{n_{\mathrm{F}}[\beta(sE-\sigma\frac{\Omega}{2})]-n_{\mathrm{F}}[\beta(sE-\omega-\sigma\frac{\Omega}{2})]}{\omega}. \tag{C61}$$

These integrals can be computed analytically. For this purpose, we first notice that the function in the integrand

$$\Theta[E-s\omega-m_f]-\Theta[-E+s\omega-m_f] = \begin{cases}+1, & E > s\omega+m_f, \\ 0, & s\omega-m_f < E < s\omega+m_f, \\ -1, & E < s\omega-m_f.\end{cases} \tag{C62}$$

In addition, the lower integration limit imposes the condition $E \geq m_f$. Therefore, if we define the index function

$$f_s(E,\omega) = \theta[E-m_f]\cdot\{\Theta[E-s\omega-m_f]-\Theta[-E+s\omega-m_f]\}, \tag{C63}$$

we obtain the following explicit expressions for $s = \pm$, respectively:

For $\omega > 2m_f$, we have

$$f_+(E,\omega) = \begin{cases}+1, & E > m_f+\omega, \\ 0, & \omega-m_f < E < \omega+m_f, \\ -1, & m_f < E < -m_f+\omega, \\ 0, & E < m_f,\end{cases} \tag{C64}$$

while for $\omega < 2m_f$,

$$f_+(E,\omega) = \begin{cases}+1, & E > m_f+\omega, \\ 0, & E < m_f+\omega.\end{cases} \tag{C65}$$

On the other hand, for $s=-1$, we obtain

$$f_{-}(E,\omega)=\begin{cases}+1, & E>m_f,\\ 0, & E<m_f.\end{cases} \tag{C66}$$

Therefore, the integral expression for $\mathcal{F}(\beta,\omega,\Omega)$ can be written as

$$\begin{aligned}\mathcal{F}(\beta,\omega,\Omega)&=\sum_{\sigma=\pm1}\sum_{s=\pm1}\int_0^\infty dE f_s(E,\omega)\Delta n_F(sE,\omega,\sigma\Omega)\\&=\sum_{\sigma=\pm1}\left\{\Theta(\omega-2m_f)\left[\int_{m_f+\omega}^\infty dE\Delta n_F(E,\omega,\sigma\Omega)-\int_{m_f}^{\omega-m_f}dE\Delta n_F(E,\omega,\sigma\Omega)\right]\right.\\&\left.+\Theta(2m_f-\omega)\int_{m_f+\omega}^\infty dE\Delta n_F(E,\omega,\sigma\Omega)+\int_{m_f}^\infty dE\Delta n_F(-E,\omega,\sigma\Omega)\right\}.\end{aligned} \tag{C67}$$

The integrals to be solved are of the general form (for suitable limits A and B)

$$\begin{aligned}\int_A^B dE n_F[\beta(sE-b)]&=\int_A^B dE\frac{e^{-\beta(sE-b)}}{1+e^{-\beta(sE-b)}}=-\frac{1}{\beta s}\ln\left[1+e^{-\beta(sE-b)}\right]\Big|_A^B\\&=\frac{1}{\beta s}\ln\left[\frac{1+e^{-\beta(sA-b)}}{1+e^{-\beta(sB-b)}}\right],\end{aligned} \tag{C68}$$

and moreover, for the explicit integrand involved in Eq. (C67) we have

$$\int_A^B dE\Delta n_F(sE,\omega,\sigma\Omega)=\frac{1}{\omega\beta s}\ln\left[\frac{1+e^{-\beta(sA-\frac{\sigma\Omega}{2})}}{1+e^{-\beta(sA-\omega-\frac{\sigma\Omega}{2})}}\frac{1+e^{-\beta(sB-\omega-\frac{\sigma\Omega}{2})}}{1+e^{-\beta(sB-\frac{\sigma\Omega}{2})}}\right]. \tag{C69}$$

Applying this basic formula, along with the identity $1+e^{-z}=2e^{-z/2}\cosh(z/2)$, we obtain

$$\begin{aligned}\mathcal{F}(\beta,\omega,\Omega)=\frac{1}{\beta\omega}\sum_{\sigma=\pm1}\left\{\Theta(2m_f-\omega)\ln\left[\frac{e^{-\frac{\beta\omega}{2}}\cosh\left[\frac{\beta}{2}\left(m_f-\frac{\sigma\Omega}{2}+\omega\right)\right]}{\cosh\left[\frac{\beta}{2}\left(m_f-\frac{\sigma\Omega}{2}\right)\right]}\right]-\ln\left[\frac{e^{-\frac{\beta\omega}{2}}\cosh\left[\frac{\beta}{2}\left(m_f+\frac{\sigma\Omega}{2}\right)\right]}{\cosh\left[\frac{\beta}{2}\left(m_f+\frac{\sigma\Omega}{2}+\omega\right)\right]}\right]\right.\\\left.+\Theta(\omega-2m_f)\ln\left[\frac{e^{-\frac{\beta\omega}{2}}\cosh\left[\frac{\beta}{2}\left(m_f-\frac{\sigma\Omega}{2}+\omega\right)\right]\cosh\left[\frac{\beta}{2}\left(m_f-\frac{\sigma\Omega}{2}-\omega\right)\right]\cosh\left[\frac{\beta}{2}\left(m_f+\frac{\sigma\Omega}{2}-\omega\right)\right]}{\cosh^2\left[\frac{\beta}{2}\left(m_f-\frac{\sigma\Omega}{2}\right)\right]\cosh\left[\frac{\beta}{2}\left(m_f+\frac{\sigma\Omega}{2}\right)\right]}\right]\right\}.\end{aligned} \tag{C70}$$

By further applying the identity $\Theta(z)+\Theta(-z)=1$ to absorb the second term into the first and third ones, respectively, we obtain

$$\begin{aligned}\mathcal{F}(\beta,\omega,\Omega)=\frac{1}{\beta\omega}\sum_{\sigma=\pm1}\left\{\Theta(2m_f-\omega)\ln\left[\frac{\cosh\left[\frac{\beta}{2}\left(m_f-\frac{\sigma\Omega}{2}+\omega\right)\right]\cosh\left[\frac{\beta}{2}\left(m_f+\frac{\sigma\Omega}{2}+\omega\right)\right]}{\cosh\left[\frac{\beta}{2}\left(m_f-\frac{\sigma\Omega}{2}\right)\right]\cosh\left[\frac{\beta}{2}\left(m_f+\frac{\sigma\Omega}{2}\right)\right]}\right]\right.\\\left.+\Theta(\omega-2m_f)\ln\left[\frac{\cosh\left[\frac{\beta}{2}\left(m_f-\frac{\sigma\Omega}{2}+\omega\right)\right]\cosh\left[\frac{\beta}{2}\left(m_f-\frac{\sigma\Omega}{2}-\omega\right)\right]\cosh\left[\frac{\beta}{2}\left(m_f+\frac{\sigma\Omega}{2}-\omega\right)\right]\cosh\left[\frac{\beta}{2}\left(m_f+\frac{\sigma\Omega}{2}+\omega\right)\right]}{\cosh^2\left[\frac{\beta}{2}\left(m_f-\frac{\sigma\Omega}{2}\right)\right]\cosh^2\left[\frac{\beta}{2}\left(m_f+\frac{\sigma\Omega}{2}\right)\right]}\right]\right\}.\end{aligned} \tag{C71}$$

Clearly, the expression above is *even* in the index $\sigma=\pm$, and hence the final result becomes

$$\mathcal{F}(\beta,\omega,\Omega)$$
$$= \Theta(2m_f-\omega)\frac{2}{\beta\omega}\ln\left[\frac{\cosh\left[\frac{\beta}{2}\left(m_f-\frac{\Omega}{2}+\omega\right)\right]\cosh\left[\frac{\beta}{2}\left(m_f+\frac{\Omega}{2}+\omega\right)\right]}{\cosh\left[\frac{\beta}{2}\left(m_f-\frac{\Omega}{2}\right)\right]\cosh\left[\frac{\beta}{2}\left(m_f+\frac{\Omega}{2}\right)\right]}\right]$$
$$+\Theta(\omega-2m_f)\frac{2}{\beta\omega}\ln\left[\frac{\cosh\left[\frac{\beta}{2}\left(m_f-\frac{\Omega}{2}+\omega\right)\right]\cosh\left[\frac{\beta}{2}\left(m_f-\frac{\Omega}{2}-\omega\right)\right]\cosh\left[\frac{\beta}{2}\left(m_f+\frac{\Omega}{2}-\omega\right)\right]\cosh\left[\frac{\beta}{2}\left(m_f+\frac{\Omega}{2}+\omega\right)\right]}{\cosh^2\left[\frac{\beta}{2}\left(m_f-\frac{\Omega}{2}\right)\right]\cosh^2\left[\frac{\beta}{2}\left(m_f+\frac{\Omega}{2}\right)\right]}\right]. \quad \text{(C72)}$$

Let us now consider the calculation of $\mathcal{G}(\beta,\omega,\Omega)$. For this purpose, we remark that the function in the integrand is given in this second case by

$$\Theta[E-s(\omega+\sigma\Omega)-m_f]-\Theta[-E+s(\omega+\sigma\Omega)-m_f]=\begin{cases}+1, & E>s(\omega+\sigma\Omega)+m_f,\\ 0, & s(\omega+\sigma\Omega)-m_f<E<s(\omega+\sigma\Omega)+m_f,\\ -1, & E<s(\omega+\sigma\Omega)-m_f.\end{cases} \quad \text{(C73)}$$

As in the former case, the lower integration limit imposes the condition $E\geq m_f$. Therefore, we define the index function

$$f_s(E,\omega+\sigma\Omega)=\theta[E-m_f]\cdot\{\Theta[E-s(\omega+\sigma\Omega)-m_f]-\Theta[-E+s(\omega+\sigma\Omega)-m_f]\}. \quad \text{(C74)}$$

In this second case, we must take into account the possibility that, for $\sigma=-1$, we may reach conditions where $\omega-\Omega<0$. Therefore, explicit expressions for the case $s=+1$ are as follows:

For $\omega+\sigma\Omega>2m_f$,

$$f_+(E,\omega+\sigma\Omega)=\begin{cases}+1, & E>m_f+\omega+\sigma\Omega,\\ 0, & -m_f+\omega+\sigma\Omega<E<m_f+\omega+\sigma\Omega,\\ -1, & m_f<E<-m_f+\omega+\sigma\Omega,\\ 0, & E<m_f,\end{cases} \quad \text{(C75)}$$

while for $\omega+\sigma\Omega<2m_f$,

$$f_+(E,\omega+\sigma\Omega)=\begin{cases}+1, & E>m_+^\sigma,\\ 0, & E<m_+^\sigma.\end{cases} \quad \text{(C76)}$$

On the other hand, for the case $s=-1$, we have the following:

For $\omega+\sigma\Omega<-2m_f$,

$$f_-(E,\omega+\sigma\Omega)=\begin{cases}+1, & E>m_f-(\omega+\sigma\Omega),\\ 0, & -m_f-(\omega+\sigma\Omega)<E<m_f-(\omega+\sigma\Omega),\\ -1, & m_f<E<-m_f-(\omega+\sigma\Omega),\\ 0, & E<m_f,\end{cases} \quad \text{(C77)}$$

while for $\omega+\sigma\Omega>-2m_f$,

$$f_-(E,\omega+\sigma\Omega)=\begin{cases}+1, & E>m_-^\sigma,\\ 0, & E<m_-^\sigma,\end{cases} \quad \text{(C78)}$$

where we defined (for $s=\pm1$ and $\sigma=\pm$)

$$m_s^\sigma = \mathrm{Max}\{m_f, m_f + s(\omega + \sigma\Omega)\}. \tag{C79}$$

These four parameters are completely specified for two particular cases,

$$m_+^+ = m_f + \omega + \Omega, \tag{C80}$$

$$m_-^+ = m_f. \tag{C81}$$

Therefore, the integral expression for $\mathcal{G}(\beta,\omega,\Omega)$ can be written as

$$\begin{aligned}
\mathcal{G}(\beta,\omega,\Omega) &= \sum_{\sigma=\pm1}\sum_{s=\pm1}\int_0^\infty dE f_s(E,\omega)\Delta n_F(sE,\omega,\sigma\Omega) \\
&= \sum_{\sigma=\pm1}\left\{\int_0^\infty dE f_+(E,\omega)\Delta n_F(E,\omega,\sigma\Omega) + \int_0^\infty dE f_-(E,\omega)\Delta n_F(-E,\omega,\sigma\Omega)\right\} \\
&= \sum_{\sigma=\pm1}\left\{\Theta(\omega+\sigma\Omega-2m_f)\left[\int_{m_f+\omega+\sigma\Omega}^\infty dE\Delta n_F(E,\omega,\sigma\Omega) - \int_{m_f}^{\omega+\sigma\Omega-m_f} dE\Delta n_F(E,\omega,\sigma\Omega)\right]\right. \\
&\quad + \Theta(2m_f-\omega-\sigma\Omega)\int_{m_+^\sigma}^\infty dE\Delta n_F(E,\omega,\sigma\Omega) + \Theta(\omega+\sigma\Omega+2m_f)\int_{m_-^\sigma}^\infty dE\Delta n_F(-E,\omega,\sigma\Omega) \\
&\quad \left. + \Theta(-\omega-\sigma\Omega-2m_f)\left[\int_{m_f-(\omega+\sigma\Omega)}^\infty dE\Delta n_F(-E,\omega,\sigma\Omega) - \int_{m_f}^{-m_f-(\omega+\sigma\Omega)} dE\Delta n_F(-E,\omega,\sigma\Omega)\right]\right\}.
\end{aligned} \tag{C82}$$

Computing each of the integrals by means of Eq. (C68), and applying the identity $\Theta(-\omega-\sigma\Omega-2m_f) = 1-\Theta(2m_f+\omega+\sigma\Omega)$, we have

$$\begin{aligned}
\mathcal{G}(\beta,\omega,\Omega) = \frac{1}{\beta\omega}\sum_{\sigma=\pm1}\Bigg\{ &\Theta(\omega+\sigma\Omega-2m_f)\ln\left[\frac{e^{-\frac{\beta\omega}{2}}\cosh\left[\frac{\beta}{2}\left(m_f+\omega+\frac{\sigma\Omega}{2}\right)\right]\cosh^2\left[\frac{\beta}{2}\left(m_f-\frac{\sigma\Omega}{2}-\omega\right)\right]}{\cosh\left[\frac{\beta}{2}\left(m_f+\frac{\sigma\Omega}{2}\right)\right]\cosh^2\left[\frac{\beta}{2}\left(m_f-\frac{\sigma\Omega}{2}\right)\right]}\right] \\
&+ \Theta(2m_f-\omega-\sigma\Omega)\ln\left[\frac{e^{-\frac{\beta\omega}{2}}\cosh\left[\frac{\beta}{2}\left(m_+^\sigma-\frac{\sigma\Omega}{2}\right)\right]}{\cosh\left[\frac{\beta}{2}\left(m_+^\sigma-\omega-\frac{\sigma\Omega}{2}\right)\right]}\right] - \Theta(2m_f+\omega+\sigma\Omega)\ln\left[\frac{e^{-\frac{\beta\omega}{2}}\cosh\left[\frac{\beta}{2}\left(m_-^\sigma+\frac{\sigma\Omega}{2}\right)\right]}{\cosh\left[\frac{\beta}{2}\left(m_-^\sigma+\omega+\frac{\sigma\Omega}{2}\right)\right]}\right] \\
&- [1-\Theta(2m_f+\sigma\Omega+\omega)]\ln\left[\frac{e^{-\frac{\beta\omega}{2}}\cosh\left[\frac{\beta}{2}\left(m_f-\omega-\frac{\sigma\Omega}{2}\right)\right]\cosh^2\left[\frac{\beta}{2}\left(m_f+\frac{\sigma\Omega}{2}+\omega\right)\right]}{\cosh\left[\frac{\beta}{2}\left(m_f-\frac{\sigma\Omega}{2}\right)\right]\cosh^2\left[\frac{\beta}{2}\left(m_f+\frac{\sigma\Omega}{2}\right)\right]}\right]\Bigg\}.
\end{aligned} \tag{C83}$$

Finally, making use of the identity $1 = \Theta(\omega+\sigma\Omega-2m_f)+\Theta(2m_f-\omega-\sigma\Omega)$, it is possible to recombine the terms above into the simplified form

$$\mathcal{G}(\beta,\omega,\Omega)=\frac{1}{\beta\omega}\sum_{\sigma=\pm1}\left\{\Theta(\omega+\sigma\Omega-2m_f)\ln\left[\frac{\cosh\left[\frac{\beta}{2}\left(m_f+\frac{\sigma\Omega}{2}\right)\right]\cosh\left[\frac{\beta}{2}\left(m_f-\frac{\sigma\Omega}{2}-\omega\right)\right]}{\cosh\left[\frac{\beta}{2}\left(m_f-\frac{\sigma\Omega}{2}\right)\right]\cosh\left[\frac{\beta}{2}\left(m_f+\frac{\sigma\Omega}{2}+\omega\right)\right]}\right]\right.$$
$$+\Theta(2m_f-\omega-\sigma\Omega)\ln\left[\frac{\cosh\left[\frac{\beta}{2}\left(m_+^\sigma-\frac{\sigma\Omega}{2}\right)\right]\cosh\left[\frac{\beta}{2}\left(m_f-\frac{\sigma\Omega}{2}\right)\right]\cosh^2\left[\frac{\beta}{2}\left(m_f+\frac{\sigma\Omega}{2}\right)\right]}{\cosh\left[\frac{\beta}{2}\left(m_+^\sigma-\omega-\frac{\sigma\Omega}{2}\right)\right]\cosh\left[\frac{\beta}{2}\left(m_f-\frac{\sigma\Omega}{2}-\omega\right)\right]\cosh^2\left[\frac{\beta}{2}\left(m_f+\frac{\sigma\Omega}{2}-\omega\right)\right]}\right]$$
$$\left.+\Theta(2m_f+\omega+\sigma\Omega)\ln\left[\frac{\cosh\left[\frac{\beta}{2}\left(m_f-\omega-\frac{\sigma\Omega}{2}\right)\right]\cosh^2\left[\frac{\beta}{2}\left(m_f+\frac{\sigma\Omega}{2}+\omega\right)\right]\cosh\left[\frac{\beta}{2}\left(m_-^\sigma+\frac{\sigma\Omega}{2}+\omega\right)\right]}{\cosh\left[\frac{\beta}{2}\left(m_f-\frac{\sigma\Omega}{2}\right)\right]\cosh^2\left[\frac{\beta}{2}\left(m_f+\frac{\sigma\Omega}{2}\right)\right]\cosh\left[\frac{\beta}{2}\left(m_-^\sigma+\frac{\sigma\Omega}{2}\right)\right]}\right]\right\}. \tag{C84}$$

APPENDIX D: THE LIMIT $\Omega=0$

In this appendix, we shall compare the limit of our analytical expression for the rate, with the result obtained by Weldon [56] for the Fermion propagator coupled to a Yukawa scalar field, that we quote as follows [see Eq. (2.22) in [56]]:

$$\mathrm{Im}\,\Pi(\omega,T)=\frac{\mathrm{i}}{2}\mathrm{Disc}\Pi(\omega,T)=\frac{g^2}{2}\int\frac{d^3k}{(2\pi)^3}\frac{N}{2E_1 2E_2}\Big[\delta(\omega-E_1-E_2)[(1-n_1)(1-n_2)-n_1n_2]$$
$$-\delta(\omega+E_1-E_2)[n_1(1-n_2)-n_2(1-n_1)]-\delta(\omega-E_1+E_2)[n_2(1-n_1)-n_1(1-n_2)]$$
$$+\delta(\omega+E_1+E_2)[n_1n_2-(1-n_1)(1-n_2)]\Big], \tag{D1}$$

with $E_1\equiv E_{\mathbf{k}}=\sqrt{m_f^2+\mathbf{k}^2}$, $E_2\equiv E_{kp}=\sqrt{m_f^2+(\mathbf{k}-\mathbf{p})^2}$, and $n_j\equiv n_F(\beta E_j)$, respectively. Since Eq. (D1) corresponds to the result for Fermions coupled to a Yukawa scalar theory [56], the overall coefficient will differ from ours due to the Dirac traces involved. Nevertheless, the expression in brackets that contains the statistical factors for the four possible microscopic processes involved is the same as in our case, as we show next.

Let us start from our expression for the imaginary part of the (contracted) polarization tensor that leads to the rate, and take the limit $\Omega\to0$ therein,

$$\lim_{\Omega\to0}\mathrm{Im}\,[g_{\mu\nu}\Pi_R^{\mu\nu}(\omega)]=4q_f^2\sum_{\sigma=\pm1}(\lim_{\Omega\to0}\mathrm{Im}[\mathcal{I}_\sigma]+\lim_{\Omega\to0}\mathrm{Im}[\mathcal{J}_\sigma])$$
$$=-\pi q_f^2m_f^2\int\frac{d^3k}{(2\pi)^3}\sum_{s=\pm1}\left\{\frac{n_{\mathrm{F}}[\beta sE_k]}{E_{kp}E_k}\Big(\delta[\omega-s(E_k-E_{kp})]-\delta[\omega-s(E_k+E_{kp})]\right)$$
$$\left.-\frac{n_{\mathrm{F}}[\beta sE_{kp}]}{E_kE_{kp}}(\delta[\omega-s(E_k-E_{kp})]-\delta[\omega+s(E_{kp}+E_k)]\Big)\right\}, \tag{D2}$$

where we used that $\lim_{\Omega\to0}\mathrm{Im}\,\mathcal{I}_\sigma=0$ after Eq. (C36), and we computed the corresponding limit $\lim_{\Omega\to0}\mathrm{Im}\,\mathcal{J}_\sigma$ from Eq. (C48). In order to compare with [56], let us switch to the notations $E_k=E_1$ and $E_{kp}=E_2$, such that after performing the sum over $s=\pm1$ explicitly in Eq. (D2) we obtain

$$\lim_{\Omega\to0}\mathrm{Im}\,[g_{\mu\nu}\Pi_R^{\mu\nu}(\omega)]=-\pi q_f^2m_f^2\int\frac{d^3k}{(2\pi)^3}\left\{\frac{n_{\mathrm{F}}[\beta E_1]}{E_1E_2}(\delta[\omega-E_1+E_2]-\delta[\omega-E_1-E_2])\right.$$
$$+\frac{n_{\mathrm{F}}[-\beta E_1]}{E_1E_2}(\delta[\omega+E_1-E_2]-\delta[\omega+E_1+E_2])-\frac{n_{\mathrm{F}}[\beta E_2]}{E_1E_2}(\delta[\omega-E_1+E_2]-\delta[\omega+E_1+E_2])$$
$$\left.-\frac{n_{\mathrm{F}}[-\beta E_2]}{E_1E_2}(\delta[\omega+E_1-E_2]-\delta[\omega-E_1-E_2])\right\}. \tag{D3}$$

Now, in order to compare with [56], let us change the notations to (for $j = 1, 2$)

$$n_{\mathrm{F}}[\beta E_j] = n_j,$$
$$n_{\mathrm{F}}[-\beta E_j] = 1 - n_{\mathrm{F}}[\beta E_j] = 1 - n_j, \tag{D4}$$

and after factoring out the delta functions in Eq. (D3), we arrive at

$$\lim_{\Omega\to 0} \mathrm{Im}\,[g_{\mu\nu}\Pi_R^{\mu\nu}(\omega)] = -\pi q_f^2 m_f^2 \int \frac{d^3k}{(2\pi)^3}\frac{1}{E_1E_2}\Big\{(n_1-n_2)\delta(\omega-E_1+E_2) - (1-n_1-n_2)\delta(\omega+E_1+E_2)$$
$$+ (n_2-n_1)\delta(\omega+E_1-E_2) + (1-n_2-n_1)\delta(\omega-E_1-E_2)\Big\}. \tag{D5}$$

Substituting the following elementary identities:

$$n_1 - n_2 = n_1(1-n_2) - n_2(1-n_1),$$
$$1 - n_1 - n_2 = (1-n_1)(1-n_2) - n_1n_2, \tag{D6}$$

into Eq. (D5), we finally arrive at

$$\lim_{\Omega\to 0} \mathrm{Im}\,[g_{\mu\nu}\Pi_R^{\mu\nu}(\omega)] = -\pi q_f^2 m_f^2 \int \frac{d^3k}{(2\pi)^3}\frac{1}{E_1E_2}\Big\{\delta(\omega-E_1-E_2)[(1-n_1)(1-n_2) - n_1n_2]$$
$$- \delta(\omega+E_1-E_2)[n_1(1-n_2) - n_2(1-n_1)] - \delta(\omega-E_1+E_2)[n_2(1-n_1) - n_1(1-n_2)]$$
$$+ \delta(\omega+E_1+E_2)[n_1n_2 - (1-n_1)(1-n_2)]\Big\}, \tag{D7}$$

where it is evident by inspection that the integrand in curly brackets is the same as in the expression reported by Weldon [56], as quoted in Eq. (D1), as we claimed.

[1] Stillman Drake, *Galileo at Work: His Scientific Biography* (Courier Corporation, Chicago, 2003).

[2] V. Voronyuk, V. D. Toneev, W. Cassing, E. L. Bratkovskaya, V. P. Konchakovski, and S. A. Voloshin, Electromagnetic field evolution in relativistic heavy-ion collisions, Phys. Rev. C **83**, 054911 (2011).

[3] Adam Bzdak and Vladimir Skokov, Event-by-event fluctuations of magnetic and electric fields in heavy ion collisions, Phys. Lett. B **710**, 171 (2012).

[4] Jorge David Castaño-Yepes, Effects of intense magnetic fields, high temperature and density on QCD-related phenomena, arXiv:2103.12898.

[5] Prabal Adhikari *et al.*, Strongly interacting matter in extreme magnetic fields, Prog. Part. Nucl. Phys. **146**, 104199 (2026).

[6] Prabal Adhikari *et al.*, Strongly interacting matter in extreme magnetic fields, arXiv:2412.18632.

[7] F. Becattini, F. Piccinini, and J. Rizzo, Angular momentum conservation in heavy ion collisions at very high energy, Phys. Rev. C **77**, 024906 (2008).

[8] F. Becattini, G. Inghirami, V. Rolando, A. Beraudo, L. Del Zanna, A. De Pace, M. Nardi, G. Pagliara, and V. Chandra, A study of vorticity formation in high energy nuclear collisions, Eur. Phys. J. C **75**, 406 (2015).

[9] Wei-Tian Deng and Xu-Guang Huang, Vorticity in heavy-ion collisions, Phys. Rev. C **93**, 064907 (2016).

[10] L. P. Csernai, V. K. Magas, and D. J. Wang, Flow vorticity in peripheral high-energy heavy-ion collisions, Phys. Rev. C **87**, 034906 (2013).

[11] L. P. Csernai, D. J. Wang, and T. Csörgő, Rotation in an exact hydrodynamical model, Phys. Rev. C **90**, 024901 (2014).

[12] STAR Collaboration, Global Λ hyperon polarization in nuclear collisions, Nature (London) **548**, 62 (2017).

[13] Anping Huang, Duan She, Shuzhe Shi, Mei Huang, and Jinfeng Liao, Dynamical magnetic fields in heavy-ion collisions, Phys. Rev. C **107**, 034901 (2023).

[14] L. A. Hernández and R. Zamora, Vortical effects and the critical end point in the linear sigma model coupled to quark, Phys. Rev. D **111**, 036003 (2025).

[15] I. I. Gaspar, L. A. Hernández, and R. Zamora, Chiral symmetry restoration in a rotating medium, Phys. Rev. D **108**, 094020 (2023).

[16] Jian-hua Gao, Bin Qi, and Shou-Yu Wang, Vorticity and magnetic field production in relativistic ideal fluids, Phys. Rev. D **90**, 083001 (2014).

[17] Barbara Betz, Miklos Gyulassy, and Giorgio Torrieri, Polarization probes of vorticity in heavy ion collisions, Phys. Rev. C **76**, 044901 (2007).
[18] Xu-Guang Huang, Pasi Huovinen, and Xin-Nian Wang, Quark polarization in a viscous quark-gluon plasma, Phys. Rev. C **84**, 054910 (2011).
[19] Minghua Wei, Yin Jiang, and Mei Huang, Mass splitting of vector mesons and spontaneous spin polarization under rotation*, Chin. Phys. C **46**, 024102 (2022).
[20] L. Adamczyk *et al.* (STAR Collaboration), Measurements of dielectron production in Au + Au collisions at $\sqrt{s_{NN}} =$ 200 GeV from the STAR experiment, Phys. Rev. C **92**, 024912 (2015).
[21] S. Acharya *et al.* (A Large Ion Collider Experiment Collaboration), Soft-dielectron excess in proton-proton collisions at $\sqrt{s} = 13$ TeV, Phys. Rev. Lett. **127**, 042302 (2021).
[22] J. Adam *et al.* (STAR Collaboration), Low-p_T e^+e^- pair production in Au + Au collisions at $\sqrt{s_{NN}} = 200$ GeV and U + U collisions at $\sqrt{s_{NN}} = 193$ GeV at STAR, Phys. Rev. Lett. **121**, 132301 (2018).
[23] Rajkumar Mondal, Nilanjan Chaudhuri, Snigdha Ghosh, Sourav Sarkar, and Pradip Roy, Dilepton production from hot and magnetized hadronic matter, Phys. Rev. D **107**, 036017 (2023).
[24] Kevin Dusling and Shu Lin, Dilepton production from a viscous QGP, Nucl. Phys. **A809**, 246 (2008).
[25] Stefano Ivo Finazzo and Romulo Rougemont, Thermal photon, dilepton production, and electric charge transport in a baryon rich strongly coupled QGP from holography, Phys. Rev. D **93**, 034017 (2016).
[26] Mauricio Martinez and Michael Strickland, Dilepton production as a measure of QGP thermalization time, J. Phys. G **35**, 104162 (2008).
[27] S. Somorendro Singh and Yogesh Kumar, Dilepton production in thermal-dependent baryonic quark–gluon plasma, Can. J. Phys. **92**, 31 (2014).
[28] Aritra Das, Aritra Bandyopadhyay, and Chowdhury Aminul Islam, Lepton pair production from a hot and dense QCD medium in the presence of an arbitrary magnetic field, Phys. Rev. D **106**, 056021 (2022).
[29] Xinyang Wang and Igor A. Shovkovy, Rate and ellipticity of dilepton production in a magnetized quark-gluon plasma, Phys. Rev. D **106**, 036014 (2022).
[30] Aritra Bandyopadhyay and S. Mallik, Effect of magnetic field on dilepton production in a hot plasma, Phys. Rev. D **95**, 074019 (2017).
[31] Kirill Tuchin, Magnetic contribution to dilepton production in heavy-ion collisions, Phys. Rev. C **88**, 024910 (2013).
[32] Rajkumar Mondal, Nilanjan Chaudhuri, Snigdha Ghosh, Sourav Sarkar, and Pradip Roy, Ellipticity of dilepton production from a hot and magnetized hadronic medium, Eur. Phys. J. A **59**, 287 (2023).
[33] Jorge David Castaño Yepes and Enrique Muñoz, Anisotropic photon and dilepton yield in a thermalized quark-gluon plasma under spatial magnetic fluctuations, Phys. Rev. D **111**, 076028 (2025).
[34] N. Sadooghi and F. Taghinavaz, Dilepton production rate in a hot and magnetized quark–gluon plasma, Ann. Phys. (Amsterdam) **376**, 218 (2017).
[35] Snigdha Ghosh and Vinod Chandra, Electromagnetic spectral function and dilepton rate in a hot magnetized QCD medium, Phys. Rev. D **98**, 076006 (2018).
[36] Snigdha Ghosh, Nilanjan Chaudhuri, Sourav Sarkar, and Pradip Roy, Effects of the anomalous magnetic moment of quarks on the dilepton production from hot and dense magnetized quark matter using the NJL model, Phys. Rev. D **101**, 096002 (2020).
[37] Nilanjan Chaudhuri, Snigdha Ghosh, Sourav Sarkar, and Pradip Roy, Dilepton production from magnetized quark matter with an anomalous magnetic moment of the quarks using a three-flavor PNJL model, Phys. Rev. D **103**, 096021 (2021).
[38] Minghua Wei, Chowdhury Aminul Islam, and Mei Huang, Production rate and ellipticity of lepton pairs from a rotating hot and dense QCD medium, Phys. Rev. D **105**, 054014 (2022).
[39] Aritra Das, Quark propagator and di-lepton production rate in a hot, dense and very strongly magnetized rotating quark-gluon plasma, arXiv:2310.11869.
[40] Alejandro Ayala, L. A. Hernández, K. Raya, and R. Zamora, Fermion propagator in a rotating environment, Phys. Rev. D **103**, 076021 (2021).
[41] Alejandro Ayala, L. A. Hernández, K. Raya, and R. Zamora, Erratum: Fermion propagator in a rotating environment [Phys. Rev. D 103, 076021 (2021)], Phys. Rev. D **104**, 039901(E) (2021).
[42] Victor E. Ambruş and Elizabeth Winstanley, Rotating fermions inside a cylindrical boundary, Phys. Rev. D **93**, 104014 (2016).
[43] Alexander Vilenkin, Quantum field theory at finite temperature in a rotating system, Phys. Rev. D **21**, 2260 (1980).
[44] Alejandro Ayala, Jorge David Castaño Yepes, M. Loewe, and Enrique Muñoz, Gluon polarization tensor in a magnetized medium: Analytic approach starting from the sum over landau levels, Phys. Rev. D **101**, 036016 (2020).
[45] Xinyang Wang, Igor A. Shovkovy, Lang Yu, and Mei Huang, Ellipticity of photon emission from strongly magnetized hot QCD plasma, Phys. Rev. D **102**, 076010 (2020).
[46] Alejandro Ayala, Jorge David Castaño-Yepes, C. A. Dominguez, S. Hernández-Ortiz, L. A. Hernández, M. Loewe, D. Manreza-Paret, and R. Zamora, Thermal corrections to the gluon magnetic Debye mass, Rev. Mex. Fís. **66**, 446 (2020).
[47] Alejandro Ayala, Jorge David Castaño-Yepes, L. A. Hernández, Jordi Salinas San Martín, and R. Zamora, Gluon polarization tensor and dispersion relation in a weakly magnetized medium, Eur. Phys. J. A **57**, 140 (2021).
[48] Xinyang Wang and Igor A. Shovkovy, Photon and dilepton emission anisotropy for a magnetized quark-gluon plasma, Phys. Rev. D **109**, 056008 (2024).
[49] Jorge David Castaño Yepes and Enrique Muñoz, Exploring magnetic fluctuation effects in QED gauge fields: Implications for mass generation, Phys. Rev. D **109**, 056007 (2024).
[50] J. Adam *et al.* (STAR Collaboration), Global polarization of Λ hyperons in au + au collisions at $\sqrt{s_{NN}} = 200$ GeV, Phys. Rev. C **98**, 014910 (2018).

[51] Lihua Dong and Shu Lin, Dilepton helical production in a vortical quark-gluon plasma, Eur. Phys. J. A **58**, 176 (2022).
[52] OpenAI, ChatGPT: Language model developed by OpenAI, https://chat.openai.com (2024).
[53] Markus Hohenwarter and GeoGebra Team, Geogebra 3D Calculator—mathematics software (2025), https://www.geogebra.org/3d?lang=en.
[54] S. Weinberg, *Gravitation and Cosmology* (Wiley, New York, 1972).
[55] N. D. Birrell and P. C. W. Davies, *Quantum Fields in Curved Space* (Cambridge University Press, Cambridge, England, 1984).
[56] H. Arthur Weldon, Simple rules for discontinuities in finite-temperature field theory, Phys. Rev. D **28**, 2007 (1983).
[57] Oleg Teryaev and Rahim Usubov, Vorticity and hydrodynamic helicity in heavy-ion collisions in the hadron-string dynamics model, Phys. Rev. C **92**, 014906 (2015).
[58] Yu. B. Ivanov and A. A. Soldatov, Vorticity in heavy-ion collisions at the JINR Nuclotron-based Ion Collider Facility, Phys. Rev. C **95**, 054915 (2017).
[59] C. Itzykson and J.-B. Zuber, *Quantum Field Theory* (Dover Publications, Inc., New York, 1980).